Characterization of phenolic compounds in green and red oak-leaf lettuce cultivars by UHPLC-DAD-ESI-QToF/MS using MS^E scan mode

Gabriela E. Viacava,[a] Sara I. Roura,[a] Luis A. Berrueta,[b] Carmen Iriondo,[b] Blanca Gallo[b] and Rosa M. Alonso-Salces[c*]

[a] Grupo de Investigación en Ingeniería en Alimentos, CONICET, Departamento de Ingeniería Química y en Alimentos, Facultad de Ingeniería, Universidad Nacional de Mar del Plata, Juan B. Justo 4302, 7600 Mar del Plata, Argentina.

[b] Grupo de Investigación de Química Analítica de Productos Naturales, Departamento de Química Analítica, Facultad de Ciencia y Tecnología, Universidad del País Vasco/Euskal Herriko Unibertsitatea (UPV/EHU), P.O. Box 644, 48080 Bilbao, Spain.

[c] Departamento de Biología, CONICET, Facultad de Ciencias Exactas y Naturales, Universidad Nacional de Mar del Plata, Funes 3350, 7600 Mar del Plata, Argentina.

* Corresponding author:

Email address: rosamaria.alonsosalces@gmail.com

This article has been accepted for publication and undergone full peer review but has not been through the copyediting, typesetting, pagination and proofreading process which may lead to differences between this version and the Version of Record. Please cite this article as doi: 10.1002/jms.4021

ABSTRACT

Lettuce (*Lactuca sativa*) is one of the most popular leafy vegetables in the world and constitutes a major dietary source of phenolic compounds with health promoting properties. In particular, the demand for green and red oak-leaf lettuces have considerably increased in the last years but few data on their polyphenol composition is available. Moreover, the utilization of analytical edge technology can provide new structural information and allow the identification of unknown polyphenols. In the present study the phenolic profiles of green and red oak-leaf lettuce cultivars were exhaustively characterized by ultrahigh performance liquid chromatography (UHPLC) coupled online to diode array detection (DAD), electrospray ionization (ESI) and quadrupole time-of-flight mass spectrometry (QToF/MS), using the MS^E instrument acquisition mode for recording simultaneously exact masses of precursor and fragment ions. One hundred fifteen phenolic compounds were identified in the acidified hydromethanolic extract of freeze-dried lettuce leaves. Forty eight of these compounds were tentatively identified for the first time in lettuce, and only twenty of them have been previously reported in oak leaf lettuce cultivars in literature. Both oak leaf lettuce cultivars presented similar phenolic composition, except for apigenin-glucuronide and dihydroxybenzoic acid, only detected in the green cultivar; and for luteolin-hydroxymalonylhexoside, an apigenin conjugate with molecular formula $C_{40}H_{54}O_{19}$ (monoisotopic MW = 838.3259 *u*), cyanidin-3-*O*-glucoside, cyanidin-3-*O*-(3"-*O*-malonyl)glucoside, cyanidin-3-*O*-(6"-*O*-malonyl)glucoside and cyanidin-3-*O*-(6"-*O*-acetyl)glucoside, only found in the red cultivar. The UHPLC-DAD-ESI-QToF/MS^E approach demonstrated to be a useful tool for the characterization of phenolic compounds in complex plant matrices.

Keywords: *Lactuca sativa*; UHPLC-QToF; mass spectrometry; polyphenol; anthocyanin; coumarin; hydrolysable tannin; lignan

Introduction

A diet rich in fruits and vegetables is associated with a reduced risk of chronic pathologies such as cancer and cardiovascular diseases.[1] This protective effect is related to polyphenols, molecules which have antioxidant activity and can reduce oxidative stress mechanisms.[2] Lettuce (*Lactuca sativa* L.) is one of the most popular leafy vegetables in the world, commonly consumed fresh in salad dishes. Lettuce contains several kinds of phenolic compounds; hydroxycinnamic acids being the most abundant class followed by flavonols, flavones, hydroxybenzoic acids and anthocyanins.[3-18] The contents of polyphenols in lettuce tissues are susceptible to high variations among cultivars and growing conditions; indeed anthocyanins have been only detected in red colored cultivars [4] and isoflavones, in iceberg lettuce.[15] Therefore, further research to characterize the polyphenolic profiles of the different lettuce varieties is fully justified. Iceberg and butterhead lettuces varieties are the most popular and predominantly used for prepared salads.[19] In particular, the demand for green and red oak-leaf lettuces have considerably increased in the last years, however few data on their polyphenol composition is available.[4] Indeed, many phenolic compounds still remain unidentified in this lettuce variety.

Regarding the analytical techniques used to characterized polyphenols in lettuce, high or ultrahigh performance liquid chromatography (HPLC or UHPLC) coupled with diode array detection (DAD) and mass spectrometry (MS and MS/MS) are the most commonly used.[3-8, 10-13, 15-17, 20, 21] UHPLC achieves rapid analysis and can obtain better peak separation than HPLC, and coupled to ToF or QToF instruments provides a highly attractive analytical technique with very high resolution and accurate mass measurements of the precursor and fragment ions.[22] This technique has been already applied to characterize 95 phenolic compounds in three lettuce cultivars (baby, romaine, and iceberg).[21] Technological advances such as the so called MS^E acquisition method maximizes the QToF instrument duty cycle,

performing simultaneous collection of precursor ions as well as other ions produced as a result of their fragmentation in exact mass mode over a single experimental run.[22] The usefulness of MS^E data acquisition mode for the identification of phenolic compounds in complex plant samples in just one injection was demonstrated by Ramirez-Ambrosi et al. (2013). In the present study, UHPLC-DAD-ESI-QToF-MS^E is used for the exhaustive characterization of the phenolic compounds contained in red and green oak-leaf lettuce cultivars.

Materials and methods

Chemicals and reagents

Water, methanol, acetonitrile, and formic acid (Fisher Scientific, Fair Lawn, NJ, USA) were of Optima® LC/MS grade; ascorbic acid (Panreac, Barcelona, Spain), analytical grade; and glacial acetic acid (Merck, Darmstadt, Germany), Suprapur® quality. Leucine Enkephalin acetate hydrate and sodium formate solution were provided by Sigma-Aldrich Chemie (Steinheim, Germany). Luteolin-7-*O*-glucoside, kaempferol-3-*O*-glucoside, quercetin-3-*O*-galactoside, quercetin-3-*O*-rhamnoside, cyanidin-3-*O*-glucoside, and cyanidin-3-*O*-galactoside were purchased from Extrasynthèse (Genay, France); caffeoyltartaric acid and quercetin-3-*O*-glucoside, from Chromadex (Irvine, CA, USA); 5-*O*-caffeoylquinic acid, *p*-coumaric acid, 1,5-dicaffeoylquinic acid, 1,3-dicaffeoylquinic acid, and quercetin-3-*O*-rutinoside, from Sigma-Aldrich Chemie (Steinheim, Germany); and ferulic acid, caffeic acid, and 3,4-dihydroxybenzoic acid, from Fluka Chemie (Steinheim,Germany). Standard stock solutions of phenolic compounds were prepared in methanol, except for anthocyanins which were prepared in methanol–HCl 30% (99:1, v/v). Dilutions from stock solutions were made in methanol-water-acetic acid (30:65:5, v/v/v).

Plant material

Two lettuce cultivars (*Lactuca sativa* L.) were studied: red oak-leaf (‘‘Krysthine RZ’’) and green oak-leaf (‘‘Versai RZ’’). Lettuces were provided by a local producer in Sierra de los Padres (Mar del Plata, Argentina), having been grown under identical agronomic field conditions following traditional standard procedures for lettuce cultivation. The leaves of ten lettuce plants of each cultivar were frozen with liquid nitrogen and freeze-dried, homogenized and crushed to obtain a homogeneous powder, which was stored at room temperature protected from light and humidity in a desiccator until analysis.

Extraction of phenolic compounds in lettuce

Freeze-dried lettuce (0.1 g) was extracted with 5 ml of methanol-water-acetic acid (30:65:5, v/v/v), containing 2 g/l of ascorbic acid to prevent polyphenol oxidation by the polyphenoloxidase enzyme, in an ultrasonic bath for 10 min. Then, the extract was centrifuged at 6000 rpm during 15 min at 4 ºC, and the supernatant was filtered through a 0.45 µm PTFE filter (Waters, Milford, CA, USA) prior to injection into the UHPLC system. Analyses were performed in triplicate.

UHPLC-DAD-ESI-QToF/MS^{E}

Lettuce extract was analyzed using an ACQUITY UPLC^{TM} system from Waters (Milford, MA, USA), equipped with a binary solvent delivery pump, an autosampler, a column compartment a PDA detector, and controlled by MassLynx v4.1 software. A reverse phase Acquity UPLC BEH C18 column (100 mm ×, 2.1 mm; particle size 1.7 µm) and a Acquity UPLC BEH C18 VanGuard^{TM} pre-column (1.7 µm) from Waters (Milford, USA) were used. Flow rate was 0.5 ml/min; injection volume, 5 µL; column and autosampler temperatures, 40ºC and 4 ºC respectively. Mobile phases consisted of 0.1% (v/v) acetic acid in water (A) and 0.1% (v/v) acetic acid in methanol (B). The elution conditions applied were: 0–8.5 min, linear gradient 0–13% B; 8.5–11 min, 13% B isocratic; 11–12.3 min, linear gradient 13–15%

B; 12.3–13.8 min, linear gradient 15–19% B; 13.8–17.3 min, linear gradient 19–23% B; 17.3–19 min, 23% B isocratic; 19–24 min, linear gradient 23–30% B; 24–26 min, 30% B isocratic; 26–27 min, linear gradient 30–100% B; 27–28 min, 100% B isocratic; and finally reconditioning of the column with 100% A isocratic. UV-visible spectra were recorded from 210 to 500 nm (20 Hz, 1.2 nm resolution). Hydroxybenzoic acids were monitored at 254 nm; flavanones at 280 nm; hydroxycinnamic acids and coumarins at 320 nm; flavonols and flavones at 370 nm; and anthocyanins at 500 nm.

All MS data acquisitions were performed on a SYNAPT^{TM} G2 HDMS with a quadrupole time of flight (QToF) configuration (Waters, Milford, MA, USA) equipped with an electrospray ionization (ESI) source operating in both positive and negative modes. The capillary voltage was set to 0.7 kV (ESI+) or 0.5 kV (ESI−). Nitrogen was used as the desolvation and cone gas at flow rates of 900 l/h and 10 l/h, respectively. The source and desolvation temperatures were 120 ºC and 400 ºC respectively. Leucine-enkephalin solution (2 ng/µL) in 0.1% (v/v) formic acid in acetonitrile-water (50:50, v/v) was used for the lock mass correction (*m/z* 556.2771 and 278.1141, or *m/z* 554.2615 and 236.1035, depending on the ionization mode, were monitored at scan time 0.2 s, interval 10 s, scans to average 3, mass window ± 0.5 Da, cone voltage 30 V, at a flow rate 10 µL/min). Data acquisition was recorded in the mass range 50–1200 *u* in resolution mode (FWHM ≈ 20,000) with a scan time of 0.2 s and an interscan delay of the 0.024 s, and automatically corrected during acquisition based on the lock mass. Before analysis, the mass spectrometer was mass calibrated with the sodium formate solution. To perform MS^{E} mode analysis, the cone voltage was set to 20 V (ESI+) or 30 V (ESI−) and the quadrupole operated in a wide band RF mode only. Two discrete and independent interleaved acquisition functions were automatically created. The first function, typically set at 6 eV in trap cell of the T-Wave, collects low energy or unfragmented data while the second function collects high energy or fragmented data

typically using 6 eV in trap cell and a collision ramp 10–40 eV in transfer cell. In both cases, Argon gas was used for Collision Induced Dissociation (CID). Data were recorded in continuous mode. For instrument control, data acquisition and processing MassLynxTM software Version 4.1 (Waters MS Technology, Milford, USA) was used.

Identification of phenolic compounds

The identification of the phenolic compounds for which standards were available was carried out by the comparison of their retention times, their UV–vis spectra and MS^E spectra recorded in positive and negative mode with those obtained by injecting standards in the same conditions. The identity of the rest of compounds was elucidated using the following analytical data: *i*) the UV–vis spectrum when it was available to assign the phenolic class,[23] since each class exhibits a characteristic UV–vis spectrum;[24] *ii*) the low collision energy MS^E spectrum in positive and negative ion mode to determine the molecular weight, since only the protonated/deprotonated molecules are able to form in the electrospray ionization source adducts, clusters and/or molecular complexes with mobile phase species, such as adducts with sodium $[M+Na]^+$ at 22 *u* above the protonated molecule, $[2M+Na]^+$ of monoacyl hydroxycinnamic acids, and the dehydrated protonated molecule ($[M+H–H_2O]^+$) of phenolic acids and diacyl hydroxycinnamic acids in positive mode, and adducts with HSO_4^- (97 *u*) and AcO^- (43 *u*) and the deprotonated dimer ion $[2M–H]^-$ of monoacyl hydroxycinnamic acid in negative mode; therefore their presence in the low collision energy spectra allows the unequivocal identification of the $[M+H]^+$ or $[M−H]^-$ ions; and *iii*) the high collision energy MS^E spectrum provides the polyphenol fragmentation patterns, which afford structural information related to the type of carbohydrates, the sequence of the glycan part, interglycosidic linkages and the aglycone moiety, allowing to assign the protonated aglycone $[Y_0]^+$ and/or the deprotonated aglycone $[Y_0]^-$. The identification of the aglycone was carried out based on the observation of $^{i,j}A^+$ and $^{i,j}B^+$ ions.[25] Furthermore, the chromatographic

elution order helped in some structural assignments, as well as bibliographic references. IUPAC nomenclature and recommended numbering system [26] were used for chlorogenic acids and flavonoids; and common names were used for other phenolic acid derivatives, coumarins, hydrolysable tannins and lignan derivatives. Structures of each family of compounds studied are presented in Fig. 1-3.

Statistical analysis

Statistical data analyses of the exact masses of protonated/deprotonated molecules and fragment ions were performed by SPSS Statistics 17.0 (IBM Corporation, Armonk, NY, 1993-2007).

Results and discussion

The phenolic compounds identified in green and red oak-leaf lettuce cultivars by UHPLC-DAD-ESI-QToF/MS^E are presented in Tables 1-3, as well as the UV-visible and MS spectral data used for their tentative identification. DAD and MS chromatograms of the green and red oak leaf lettuce cultivars are shown in Figs. 1S-4S (supplementary information). The high and low energy function MS spectra of compounds from the different phenolic families detected in these cultivars are displayed in Figs. 4-6 and Figs. 5S-8S (supplementary information).

Phenolic acid derivatives

The identification of phenolic acid derivatives, i.e. hydroxycinnamic, hydroxybenzoic and hydroxyphenylacetic derivatives, were carried out taking into account mainly the negative ion mode mass spectra; the positive ion mode being used for verification. In the high collision energy MS spectra, losses of H_2O, CO_2 and CO were regularly observed, which have also been described by other authors using IT, QqQ, and QToF.[22, 27]

Hydroxycinnamic derivatives

Caffeoylquinic acids. Three major chromatographic peaks (**1, 3, 6**), presenting the same UV spectra as the standard *trans*-5-caffeoylquinic acid (*trans*-5-CQA), were detected in the chromatograms extracted from the Total Ion Current (TIC) MS scan chromatogram in negative and positive modes at *m/z* 353 and 355 respectively, which were due to three caffeoylquinic acid (CQA) isomers (Fig. 3S in the supplementary information). Compound **3** (Rt= 7.32 min, λmax= 300, 324 nm) was identified unambiguously as *trans*-5-caffeoylquinic acid by comparison with its standard: the deprotonated molecule $[M-H]^-$ at *m/z* 353 yielded fragment ions at *m/z* 191, 173 and 135; and the protonated molecule $[M+H]^+$, at *m/z* 163 and 145 (Fig. 4). Moreover, its sodium adducts, $[M+Na]^+$ and $[2M+Na]^+$ at *m/z* 377 and 731 respectively, were also observed. Compounds **1** (Rt= 4.74 min, λmax= 301, 323 nm) and **6** (Rt= 10.23 min, λmax= 301, 316 nm) had the same fragmentation pattern as 5-CQA, and their *m/z* values for $[M+H]^+$ and $[M-H]^-$ were confirmed with the sodium adduct at *m/z* 377 in positive ionization mode, and the $[2M-H]^-$ ion at *m/z* 707 in negative mode. All three peaks (**1, 3, 6**) yielded the same base peak at *m/z* 191 due to the deprotonated quinic moiety in the negative high energy function. None of the peaks yielded an intense fragment ion at *m/z* 173 ($[\text{quinic acid}–H–H_2O]^-$). This dehydrated ion of quinic acid is characteristically formed in the negative ion mode when the cinnamoyl group is bonded to the quinic moiety at position 4, as already noted by other authors using other QqQ/MS [28] or IT/MS.[29, 30] Peak **1** also gave intense ions from the caffeoyl moiety ($[\text{caffeic acid}–H–CO_2]^-$) at *m/z* 135 (71% relative abundance (RA)) and ($[\text{caffeic acid}–H]^-$) at *m/z* 179 (32% RA), characteristic ions of the fragmentation pattern of 3-CQA by QqQ/MS.[28] The relative hydrophobicity of cinnamoyl derivatives depends on the position, the number, and the identity of the cinnamoyl residues. In general, those chlorogenic acids (CGAs) with a greater number of free equatorial hydroxyl groups in the quinic acid are more hydrophilic than those with a greater number of

free axial hydroxyl groups.[31] Taking into account the fact that the hydroxyl groups in the quinic acid are axial in position 1 and 3, and equatorial in positions 4 and 5,[30] the elution order observed for monoacyl-CGAs on endcapped C18 reversed-phase LC columns is 3-CGA, 5-CGA and 4-CGA. This empirical rule was observed by several authors.[21, 28, 29, 32] So, isomers substituted in position 3 were the most hydrophilic; and in position 4 the most hydrophobic, although in some packings 4-CQA precedes 5-CQA.[31] On the other hand, the ease of removal of the caffeoyl residue during fragmentation is 1 ≈ 5 > 3 > 4.[31] In the negative low energy function, the base peaks were $[M-H]^-$ at *m/z* 353 for peak **1**, and [quinic acid–H]$^-$ at *m/z* 191 for peaks **3** and **6**, revealing that the caffeoyl moiety in peak **1** was bonded to the quinic structure in a stronger position. So, peak **1** was tentatively assigned to a 3-CQA isomer.

Besides the three major peaks (**1, 3, 6**), other four caffeoylquinic acid isomers (**2**, Rt= 6.65 min; **4**, Rt= 8.12 min; **5**, Rt= 8.36 min; **7**, Rt= 15.06 min) were detected in the chromatograms extracted at *m/z* 353 (ESI–) and 355 (ESI+) (Fig. 3S in the supplementary information), presenting the same fragmentation pattern in the positive mode as the former isomers. Chlorogenic acid isomers 1-CQA, 3-CQA (neochlorogenic acid), *cis*-3-CQA, 4-CQA (cryptochlorogenic acid), *cis*-4-CQA and *cis*-5-CQA have been previously found in different *Asteraceae* species.[16, 31, 33] In the negative low energy function, compounds **2**, **4** and **7** yielded the deprotonated molecule $[M-H]^-$, whereas all four peaks presented the same base peak at *m/z* 191 due to the deprotonated quinic moiety in the negative high energy function. Furthermore, peak **4** yielded ions at *m/z* 135 (21% RA) and at *m/z* 179 (12% RA); and peak **5**, also at *m/z* 173 (13% RA), whereas for all other isomers, this ion was less than 4% RA. Peak **5,** presenting the most intense *m/z* 173 and eluting later than 5-CQA (**3**), was ascribed to a 4-CQA isomer.

It is widely accepted that *trans* isomers are the substrates and products of the main phenylproponanoid biosynthetic pathway, being the predominant species detected in plant tissues. However it is also known that conversion to the *cis* form occurs readily, especially after exposure to UV light, and therefore *cis* isomers might reasonably be expected in plant extracts.[34] Indeed, *cis*-3-CQA, *cis*-4-CQA and *cis*-5-CQA have been previously found in different *Asteraceae* species.[16, 31, 33] *Cis* isomers fragment identically to the more common *trans* isomers, however *cis* and *trans* isomers are easily resolved by chromatography.[34] *Cis*-5-acyl and *cis*-1-acyl CGAs are more hydrophobic, thus elute later than their *trans* isomers, whereas the opposite happens with *cis*-3-acyl and *cis*-4-acyl CGAs on endcapped C18 and phenylhexyl packings.[34-36] These observations helped to tentatively identify some compounds. Thus, peak **6** was attributed to *cis*-5-CQA, taking into account the elution order of *cis* and *trans* isomers; the fact that absorption maximum for *cis*-CGA occurs at shorter wavelength than for their *trans* form [37] and that it is a major peak as its *trans* isomer. Peaks **1** and **4**, which showed similar fragmentation patterns, were designated to the *trans* and *cis* isomers of 3-CQA respectively.

Peak **2** showed a similar fragmentation pattern to peaks **3** and **6**. Indeed, 1-CQA and 5-CQA are not possible to be reliably distinguished by their fragmentation.[31] Fortunately, *trans*-5-CQA is readily available from commercial sources, and 1-CQA can be easily resolved in the chromatographic elution from this, so, in practice, discrimination is straightforward. Peak **2** eluted earlier than *trans*-5-CQA (**3**) and was assigned to a 1-acyl isomer. The remaining peak (**7**) eluted the latest of all CQA, therefore it was ascribed to the other 4-CQA isomer.

Taking into account all the above considerations, the chromatographic peaks were tentatively identified as: **1**, *trans*-3-CQA; **2**, *trans*-1-CQA; **3**, *trans*-5-CQA; **4**, *cis*-3-CQA; **5**, *trans*-4-CQA; **6**, *cis*-5-CQA; and **7**, *cis*-4-CQA. Only three CQA isomers had been reported

previously in green lettuce, i.e. 5-CQA, 3-CQA and an unidentified CQA isomer.[11, 21] and only 5-CQA in the red oak-leaf cultivar [4, 9, 20] *trans*-5-CQA (**3**) was the major phenolic compound in both oak-leaf cultivars, as occurs in other lettuce varieties.[4, 6, 18] The following major CQAs were *cis*-5-CQA and *trans*-3-CQA (40% and 5% of the total intensity of *trans*-5-CQA respectively in the green cultivar, and about 5% for each CQA isomer in the red cultivar).

***p*-Coumaroylquinic acids.** Compounds **8** (Rt= 9.82 min, λmax= 312 nm) and **9** (Rt= 13.74 min, λmax= 308 nm) were identified as *p*-coumaroylquinic acid isomers on the basis of mass spectral data and UV spectra, which followed the pattern of the *p*-coumaric acid standard. In both low and high energy positive ion mode, the sodium adduct $[M+Na]^+$ at *m/z* 361 was the base peak for both compounds, and the ion at *m/z* 147 ($[p\text{-coumaroyl}+H]^+$) was the secondary most intense ion. In the negative low energy function, the base peaks were $[M-H]^-$ at *m/z* 337 for peak **8**, and $[\text{quinic acid}-H]^-$ at *m/z* 191 for peak **9**, revealing that the *p*-coumaroyl moiety in peak **8** was bonded to the quinic structure in a stronger position. Moreover, peak **8** yielded in the high energy function an intense ion at *m/z* 119 due to its decarboxylation product $[\text{p-coumaric acid-H-}CO_2]^-$, which is characteristic of the fragmentation pattern of 3-*p*-coumaroylquinic acid,[29] thus this isomer was tentatively assigned to peak **8,** for the first time in lettuce cultivars. The base peak of compound **9** at *m/z* 191 due to the deprotonated quinic moiety is characteristic of 5-*p*-coumaroylquinic acid.[29] Similarly to CQA isomers, the elution order of both isomers on endcapped C18 packings agrees with these tentatively assignments.[21, 28, 29, 32] 5-*p*-coumaroylquinic acid and an unidentified isomer have been previously reported in bibliography in green lettuce cultivars.[6, 21] To the authors' knowledge the presence of *p*-coumaroylquinic acids are here reported in green and red oak-leaf cultivars for the first time.

Caffeoyltartaric acid. A caffeoyltartaric acid (peak **10**: Rt= 9.06 min, λmax= 301, 323 nm) was detected in the extracted MS chromatogram set at *m/z* 311 in the negative ion mode, presenting the corresponding fragmentation pattern: The dehydrated protonated molecule at *m/z* 293 was the base peak in low energy function; and intense fragments of the deprotonated tartaric (*m/z* 149) and caffeic (*m/z* 179) acids and the losses of water (*m/z* 293) and CO_2 (*m/z* 135; base peak) were observed in the high energy function. Two isomers of caffeoyltartaric acid have been already reported in lettuce in literature,[6, 11, 12, 21, 38] also in green and red oak-leaf cultivars.[4, 39]

p-Coumaroyltartaric acid. Peak **11** (Rt= 15.63 min, λmax= 310 nm), detected in the extracted MS chromatogram set at *m/z* 295 in the negative ion mode, yielded the base peak at *m/z* 163 due to the deprotonated *p*-coumaric acid, and two fragments at *m/z* 149 (50% RA) and *m/z* 119 (60% RA) due to the deprotonated tartaric acid and the descarboxilation of *p*-coumaric acid in the low energy function. Thus, compound **11** was tentatively identified as *p*-coumaroyltartaric acid, which has been previously found in green lettuce cultivars,[6, 21] being detected here in oak-leaf cultivars for the first time.

Caffeoylmalic acid. Caffeoylmalic acid (CMA) (peak **12**: Rt= 9.05 min, λmax= 301, 323 nm) was detected when the *m/z* value for the extracted MS chromatogram was set at *m/z* 295 (negative ion mode) or 297 (positive ion mode). Besides the UV spectra of peak **12** followed the pattern of caffeic acid standard. In the negative ion mode, the high energy function provided ions corresponding to malic acid: the base peak at *m/z* 133 was due to the deprotonated malic moiety; and fragment ions, to the losses of water and CO at *m/z* 115 and 105 respectively. MS^E experiments in the positive ion mode showed that CMA behaved as described above for CQA, yielding the same ions from the caffeoyl moiety, as well as the sodium adduct. CMA, commonly named as phaseolic acid, has been described before in

different lettuce cultivars,[6, 12, 21, 38] and already detected in the red oak-leaf lettuce cultivar,[4, 9, 14] but in green oak-leaf lettuce for the first time in the present work.

Dicaffeoylquinic acids and caffeoylquinic acid glycosides. Both dicaffeoylquinic acids (diCQA) and caffeoylquinic acid-hexosides present an average molecular mass of 516 *u*, and produce isobaric deprotonated or protonated molecules at *m/z* 515 and 517 in the negative and positive ion modes respectively. Five peaks were detected in the extracted MS chromatograms at these *m/z* values: peak **13** (Rt= 5.86), peak **14** (Rt= 7.56), peak **15** (Rt= 20.20, λmax= 321 nm), peak **16** (Rt= 20.63, λmax= 326 nm) and peak **17** (Rt= 24.17, λmax= 331 nm) (Fig. 3S in the supplementary information). Based on their accurate masses and fragmentation patterns, these peaks were distinguished as either di-caffeoylquinic acids (**15**, **16** and **17**) with monoisotopic $[M-H]^-$ at *m/z* 515.1190 ($C_{25}H_{23}O_{12}$) and monoisotopic $[M+H]^+$ at *m/z* 517.1346 ($C_{25}H_{25}O_{12}$), and caffeoylquinic acid-hexosides (**13** and **14**) with monoisotopic $[M-H]^-$ at *m/z* 515.1401 ($C_{22}H_{27}O_{14}$) and monoisotopic $[M+H]^+$ at *m/z* 517.1548 ($C_{22}H_{29}O_{14}$) in the negative and positive ion modes respectively.

The first fragments of the diCQA were due to the loss of one of the caffeoyl moieties, leading to the precursor ion of a CQA; therefore, subsequent fragmentation of these ions yielded the same fragments as the corresponding CQA. In the positive low energy function, the sodium adducts at *m/z* 539 and the dehydrated protonated molecule at *m/z* 499 were detected with different % RA: peak **15**, $[M+H-H_2O]^+$ base peak and $[M+Na]^+$ 80% RA; peak **16**, $[M+Na]^+$ base peak and $[M+H-H_2O]^+$ 20% RA; and peak **17**, $[M+Na]^+$ base peak and $[M+H-H_2O]^+$ 90% RA. The positive high energy function gave a base peak at *m/z* 163 ([caffeic acid+H–H_2O]$^+$) for the three peaks, but $[M+Na]^+$ presented 50% RA for peak **15**, 35% RA for peak **16**, and 70% RA for peak **17**. The % RA differences between these ions are related to the difficulty of removing the acylating residue at the different positions.[31] In accordance with this, the negative low energy function MS spectra disclosed that peak **17**

yielded only the deprotonated molecule (*m/z* 515) as the base peak; peak **15**, the base peak $[M-H]^-$ and the fragment $[CQA-H]^-$ ion at *m/z* 353 with 65% RA; and peak **16**, the base peak $[CQA-H]^-$ at *m/z* 353 and $[M-H]^-$ with 40% RA. Hence, these observations suggest that peak **17** contains a caffeoyl moiety at the positions more difficult to be removed (4 > 3 > 5 ≈ 1) [29, 31] than the other peaks, followed by peak **15**. Indeed, the presence of the dehydrated quinic residue ion [quinic acid–H–H_2O]$^-$ at *m/z* 173 as the base peak in the high negative energy spectra of peak **17** revealed that one of the caffeoyl moieties was bonded to quinic acid at position 4. Then it remained to be determined if the other caffeoyl moiety was substituted at position 1, 3 and 5. Finally, taking also into account the elution order of diCQA isomers (retention time on endcapped C18 packings: 1,3-diCQA <<< 1,4-diCQA << 3,4-diCQA < 1,5-diCQA < 3,5-diCQA << 4,5-diCQA) reported in bibliography,[28, 31] compound **17** was assigned to 4,5-diCQA. In the high negative energy function, base peaks of compounds **15** and **16** were [quinic acid–H]$^-$ at *m/z* 191, whereas the characteristic fragment at *m/z* 173 corresponding to the dehydrated quinic residue ion was not detected. Therefore, caffeoyl moieties were substituted at position 1, 3 and 5. Compound **15** was identified unambiguously as 1,5-diCQA by comparison with its standard. Thus, regarding its retention time and the ease of removal of the caffeoyl residue, compound **16** was assigned to 3,5-diCQA. Isomers 3,5-diCQA (isochlorogenic acid A), *cis*-3,5-diCQA, and 4,5-diCQA (isochlorogenic acid B) have previously been reported in *L. sativa*.[4, 6, 21, 38, 40] Among these, isochlorogenic acid A was reported to be the most abundant in lettuce, as found in the present study, which supported the assignment of compound **16**.[6, 7, 11, 13, 38] 1-acyl CGA have been found in some Asteraceae,[31] however the isomer 1,5-diCQA is reported in lettuce here for the first time.

Caffeoylquinic acid-hexosides (**13** and **14**) base peaks were their sodium adducts in the positive ion mode and the deprotonated molecule in the negative ion mode, which confirmed

their identities. The presence of the fragment ion at *m/z* 353 due to the deprotonated CQA, and the base peak at *m/z* 191 due to the deprotonated quinic acid in the negative high energy function of peak **13** also support the assignment. Peak **14** was at trace levels, not being possible to register its fragmentation pattern. To the authors' knowledge, caffeoylquinic acid-hexosides have not been reported in lettuce before.

***p*-Coumaroylcaffeoylquinic acids.** Two chromatographic peaks showed protonated and deprotonated molecules that corresponded to *p*-coumaroylcaffeoylquinic acids, at *m/z* 501 in the positive ion mode and at *m/z* 499 in the negative mode: peak **18 (**Rt= 23.58 min, λmax= 312 nm) and peak **19** (Rt= 23.95 min, λmax= 316 nm). In the positive high energy function, the base peaks yielded by both isomers were the fragment ion at *m/z* 147 due to [*p*-coumaroyl+H]$^+$, disclosing that the *p*-coumaroyl moiety was attached to the quinic acid in a weaker position than the caffeoyl one. This was also supported by the fragmentation pattern observed for both peaks in the negative ion mode, which yielded the deprotonated molecules, and fragments at *m/z* 353 due to the loss of the *p*-coumaroyl moiety (85-95% RA) and at *m/z* 337 due to the loss of the caffeoyl moiety (40-50% RA) in the low energy function, indicating that the former loss was favored. This fragmentation pattern was reported for 3-*p*-coumaroyl-4-caffeoylquinic acid (3-*p*Co-4-CQA) and 4-caffeoyl-5-*p*-coumaroylquinic acid (4-C-5-*p*CoQA).[41] The deprotonated quinic acid ion at *m/z* 191 was the base peak in the high energy function; this fragment is a characteristic base peak of 5-CQA, 3-CQA and 5-*p*CoQA, and is yielded by 4-CQA.[29] Thus, taking also into account that the elution order on endcapped C18 packings is 3,4-isomers, 3,5-isomers and 4,5-isomers,[41] compounds **18** and **19** were tentatively assigned to 3-*p*Co-4-CQA and 4-C-5-*p*CoQA respectively, for the first time in lettuce cultivars. *p*-Coumaroylcaffeoylquinic acids have been previously reported in lettuce,[16, 21] but is the first time in green and red oak-leaf cultivars.

Dicaffeoyltartaric acids. Two peaks (**20**, **21**), presenting the same UV spectra as caffeic acid standard, were detected in the chromatograms extracted from the TIC MS scan chromatogram in positive and negative modes at *m/z* 475 and 473, respectively, which were due to two dicaffeoyltartaric acid isomers (diCTA). Compound **20** (Rt= 10.53 min, λmax= 301, 324 nm) and compound **21** (Rt= 12.54 min, λmax= 301, 323 nm) presented the same fragmentation pattern, and their identity was confirmed with the sodium adduct at *m/z* 497 in positive ionization mode and the $[2M-H]^-$ ion at *m/z* 947 in negative mode for peak **20**, and the protonated and deprotonated molecules for peak **21**. In the negative ion mode, both peaks (**20**, **21**) yielded the same base peak at *m/z* 293 due to the loss of water of the deprotonated caffeoyltartaric acid, and $[CTA–H]^-$ at *m/z* 311 due to the loss of one of the caffeoyl moieties, as well as ions from the tartaric moiety, [tartaric acid–H]$^-$ at *m/z* 149 and [tartaric acid–H–CO_2]$^-$ at *m/z* 105; and ions from the caffeoyl moiety, [caffeic acid–H]$^-$ at *m/z* 179 and [caffeic acid–H–CO_2]$^-$ at *m/z* 135. Compound **20** was tentatively identified as di-*O*-caffeoyltartaric (chicoric acid), and compound **21** as meso-di-*O*-caffeoyltartaric acid, since they were detected in lettuce elsewhere; the former being reported as the most abundant as we observed,[6, 7, 10-13, 21, 38] as well in oak-leaf cultivars.[4, 9, 14, 39]

Other hydroxycinnamic acid derivatives. Several cinnamoyl glycosides were found in the lettuce extracts, such as caffeoyl-hexosides, *p*-coumaroyl-hexosides, sinapoyl-hexosides and dihydrocaffeic acid-hexosides, whose fragmentation patterns were characterized by the aglycone product ion resulted from the loss of a hexose residue.[21, 42]

Eight peaks (**22**, Rt= 5.39 min; **23**, Rt= 5.64 min; **24**, Rt= 6.08 min, λmax= 301, 325 nm; **25**, Rt= 7.69 min; **26**, Rt= 8.44 min; **27**, Rt= 9.01 min; **28** Rt= 9.52 min; and **29** Rt= 9.64 min) were observed in the chromatogram extracted at *m/z* 343 and 341 in positive and negative ion modes respectively. All of them (**22**-**29**) produced *m/z* 179 and 135 in negative ion mode, and *m/z* 163, 145, 135, 117 and 89 in positive ion mode, consistent with the

presence of a caffeic acid residue. Thus, these compounds were tentatively assigned as isomeric caffeic acid-hexosides, in agreement with Clifford et al. (2007). Moreover, the identity of peaks **22-26** and **28** were confirmed by the presence of their sodium adducts in the positive low energy function. As well, peak **30** (Rt= 8.01 min, λmax= 301, 325 nm) showed the same fragmentation pattern as caffeic acid, yielding also a monoisotopic protonated molecule at *m/z* 359.0802 ($C_{18}H_{15}O_8$) in the positive ion mode, and a monoisotopic deprotonated molecule at *m/z* 357.0633 ($C_{18}H_{13}O_8$) in the negative ion mode. Thus, it was tentatively assigned as a caffeoyl derivative, however the nature of the non-phenolic residue (196.0387 *u*) was not able to be disclosed. Such caffeoyl derivative has not previously been reported in lettuce so far we are aware.

Similarly, four isomers of synapic acid-hexosides (**31**, Rt= 6.03 min, λmax= 301, 326 nm; **32**, Rt= 9.70 min; **33**, Rt= 10.36 min; **34**, Rt= 13.13 min) were tentatively identified in the extracted traces at *m/z* 387 and 385 in the positive and the negative ion modes respectively. Ions corresponding to the deprotonated aglycone at *m/z* 223, and the subsequent decarboxylations and losses of methyl residues at *m/z* 208, 179, 164, and 149 from the synapoyl moiety were detected in the negative ion mode. In addition, the positive ion mode yielded the sodium adduct at *m/z* 409 and ions due to the loss of the hexose residue at *m/z* 225, and subsequent losses of H_2O at *m/z* 207, CH_3OH at *m/z* 192, and CO at *m/z* 129. One isomer of synapic acid-hexoside has been previously reported in green lettuce cultivars.[21]

Following this fragmentation patterns, a *p*-coumaric acid-hexoside (**35**, Rt= 8.32 min) and two dihydrocaffeic acid-hexosides (**36**, Rt= 3.70 min; **37**, Rt= 3.83 min) were also characterized. All of them yielded the product ion due to the loss of the hexose residue (*m/z* 163 for **35**, *m/z* 181 for **36** and **27**), with the subsequent losses of H_2O, CO and CO_2 in the negative ion mode; and the sodium adduct in the positive ion mode (*m/z* 349 for **35**, *m/z* 367 for **36** and **37**).

Seven caffeic acid-hexosides, a synapic acid-hexosides, a dihydrocaffeic acid-hexoside and a *p*-coumaric acid-hexoside have been previously reported in green lettuce cultivars.[21] In the present work, one more caffeic acid-hexoside, a dihydrocaffeic acid-hexoside and three synapic acid-hexosides were identified in the red and green oak-leaf lettuce cultivars.

Peaks **38** (Rt= 11.81 min, λmax= 307 nm), **39** (Rt= 14.47 min) and **40** (Rt= 16.48 min) were tentatively proposed as isomers of ferulic acid methyl esters. According to previous data,[21, 42] these compounds showed demethylated fragment ions at *m/z* 192 ($[M–H–CH_3]^-$) and *m/z* 177 ($[M–H–2CH_3]^-$), which is characteristic of the methoxylated cinnamic acids. Two of these isomers of ferulic acid methyl esters have been previously reported in green lettuce cultivars.[21]

Hydroxybenzoic derivatives

Hydroxybenzoic derivatives were not detected in the positive ion mode. Thus, no peaks were detected in the chromatograms extracted from the TIC MS scan chromatogram at the protonated molecule or the sodium adduct masses of the hydroxybenzoic derivatives observed in the negative ion mode. Only one of the two previously reported in green lettuce cultivars [21] isomers of hydroxybenzoic acid (**41**: Rt= 4.67 min) and dihydroxybenzoic acid (**42**: Rt= 5.42 min) were detected at *m/z* 137 and *m/z* 153 respectively (Fig. 3S in the supplementary information). Their corresponding decarboxylated ions were also observed at *m/z* 93 and *m/z* 109 respectively. The dihydrobenzoic acid (**42**) was only detected in green oak-leaf lettuce cultivar.

Several hydroxybenzoic glycoside esters were characterized according to their MS data and fragmentation pattern by the neutral loss of the glycosidic moiety. Hydroxybenzoic acid-hexosides (**43**, Rt= 4.22 min; **44**, Rt= 5.15 min) yielded the deprotonated ion at *m/z* 299 and the product ions due to losses of the hexose residue (*m/z* 137) and CO_2 (*m/z* 93). Dihydroxybenzoic acid-hexosides (**45**, Rt= 2.49 min; **46**, Rt= 2.69 min; **47**, Rt= 3.74 min; **48**,

Rt= 3.91 min; **49**, Rt= 4.48 min; **50**, Rt= 4.68 min) produced the deprotonated molecule at *m/z* 315 (base peak), an odd electron product ion at *m/z* 152 corresponding to the loss of hexose plus H (163 *u*), an even electron ion at *m/z* 153 due to the loss of hexose (Fig. 3S in the supplementary information), the dehydrated ion at *m/z* 135, and the decarboxylated ion at *m/z* 109, in agreement with bibliography.[21] Hence, one more hydroxybenzoic acid-hexoside and four more dihydroxybenzoic acid-hexosides are here detected in green and red oak-leaf lettuce cultivars than in previous studies on different lettuce varieties.[43] The release of such unusual losses was also observed for gallic acid-hexoside isomers.[21] Thus, peaks **51** (Rt= 2.80 min), **52** (Rt= 2.88 min) and **53** (Rt= 6.61 min) were tentatively proposed as gallic acid-hexosides, since they yielded the deprotonated molecule at *m/z* 331 (base peak), and an odd electron product ion at *m/z* 168, corresponding to the loss of hexose plus H (163 *u*), an even electron ion at *m/z* 169 due to the loss of hexose, and [gallic acid–H–CO_2]$^-$ at *m/z* 125. Two isomers of gallic acid-hexoside have been detected previously only in the lettuce cv. baby.[21]

Aside from the loss of the hexose moiety, syringic acid-hexoside (**54**, Rt= 5.90 min, *m/z* 359) showed subsequent losses of CH_3 from the methoxy groups of the aglycone and CO_2 (*m/z* 182, 153, 138 and 123), as previously observed in literature.[21, 42]

In agreement with previous studies,[21] compounds **55** (Rt= 17.09 min) and **56** (Rt= 24.83 min), showing a deprotonated molecule at *m/z* 451, were tentatively assigned as hydroxybenzoyl-gallic acid-hexosides. The high energy function yielded the fragment ion corresponding to the deprotonated gallic acid-hexoside at *m/z* 331, after the loss of the hydroxybenzoyl moiety (120 *u*). As well, product ions due to successive losses of H_2O at *m/z* 313, hexose plus H at *m/z* 168 and CO_2 at *m/z* 124 were observed. A similar pattern was found for the hydroxybenzoyl-dihydroxybenzoic acid-hexosides (**57**, Rt= 17.68 min; **58**, Rt= 19.41 min; **59**, Rt= 23.64 min; **60**, Rt= 26.88 min, λmax= 256, 335 nm; **61**, Rt= 27.09 min) detected in the extracted trace at *m/z* 435 (Fig. 3S in the supplementary information). For

peak **59**, only the deprotonated molecule was detected due to its low concentration in the extract. All other isomers yielded the fragment ions corresponding to [dihydroxybenzoic acid-hexoside–H]$^-$ at *m/z* 315, and the subsequent losses of H_2O at *m/z* 297 and hexose plus H at *m/z* 152 and CO_2 at *m/z* 108. Peaks **58** and **61** showed the product ion [dihydroxybenzoic acid–H]$^-$ due to an even electron ion at *m/z* 153 (loss of hexose), instead of the odd electron product ion at *m/z* 152. Besides, peaks **57**, **60** and **61**, yielded the fragment ion [hydroxybenzoic acid–H]$^-$ at *m/z* 137 and its corresponding decarboxylation ion at *m/z* 93. This behavior agrees with that observed for hydroxycinnamic acid glycosides above and in literature,[33] which suggest that both, the hydroxybenzoic acid moiety and the dihydroxybenzoic acid moiety, are attached through their phenolic hydroxyl to different positions of the same hexose molecule. Just one isomer of hydroxybenzoyl-gallic acid-hexoside and two isomers of hydroxybenzoyl-dihydroxybenzoic acid-hexosides have been previously characterized only in cv. baby lettuce.[21]

Hydroxyphenylacetic derivatives

Taking into account the MS data, the fragmentation patterns observed for hydroxybenzoic acid in the negative ion mode and bibliography,[21, 42] 4-hydroxyphenylacetic acid was tentatively assigned to peak **62** (Rt= 5.60 min), which yielded the deprotonated molecule at *m/z* 151 and fragment ions due to the loss of CO at *m/z* 123 and CO_2 at *m/z* 107, showing the typical decarboxylation of phenolic acids. This compound has been previously detected in green lettuce cultivars.[21]

Flavonoids

Flavonols

Thirteen quercetin glycosides (**63**-**75**) and four kaempferol glycosides (**76**-**79**) were detected and identified on the basis of their mass spectral data (Fig. 4S in the supplementary information), comparison with available standards, and literature. Flavonol monoglycoside

mass spectra in the positive mode showed the protonated molecule $[M+H]^+$, the sodium adduct ion $[M+Na]^+$ and the protonated aglycone ion $[Y_0]^+$ as a result of the loss of the sugar or organic acid residue (losses: 146 *u*, rhamnosyl residue; 162 *u*, hexosyl residue; 176 *u*, glucuronic residue; 178 *u*, gluconic residue; 248 *u*, malonyl-hexosyl residue; 324 *u*, di-hexosyl residue; 338 *u*, glucuronic + hexosyl residue; 410 *u*, hexosyl + malonyl-hexosyl residue; 424 *u*, glucuronic + malonyl-hexosyl residue). In the mass spectrum of flavonol diglycosides, a fragment $[Y_1]^+$ due to the loss of the first sugar or organic acid unit was also observed. In the negative mode, the high energy function product ions corresponding to quercetin at *m/z* 300 (odd electron ion) and/or 301 (even electron ion) were detected, as observed in MS/MS elsewhere.[21] Regarding this, compounds **63** (Rt= 17.16 min, λmax= 279, 344 nm), **64** (Rt= 18.03 min, λmax= 252, 367 nm) and **65** (Rt= 20.25 min, λmax= 252, 330 nm) were identified as quercetin-3-*O*-hexosides on the basis of their protonated molecule at *m/z* 465 and a high energy function product ion at *m/z* 303, which indicates cleavage of a hexosyl group. This fragmentation pattern and chromatographic retention time of the reference standard confirmed that compound **65** was quercetin-3-*O*-galactoside. Two isomers of quercetin hexose have been previously described in lettuce.[4, 7-13, 20, 21, 38]

Compound **66** (Rt= 18.44 min, λmax= 254, 349 nm) was identified as quercetin-3-*O*-glucuronide because of $[M+H]^+$ at *m/z* 479, $[M+Na]^+$ at *m/z* 501 and $[Y_0]^+$ at *m/z* 303, which indicated the loss of a glucuronic residue in the positive mode. Similarly, in the negative mode, the deprotonated molecule $[M-H]^-$ at *m/z* 477 yielded $[Y_0]^-$ at *m/z* 301; the loss of 176 *u* pointed out the presence of a glucuronic residue (Fig. 5S in the supplementary information). This glucuronic group was also observed in compound **67** (Rt= 9.50 min, λmax= 256, 352 nm) and compound **68** (Rt= 10.58 min), which gave $[M+H]^+$ at *m/z* 641, $[M+Na]^+$ at *m/z* 663, and $[Y_0]^+$ at *m/z* 303 in positive mode, and peak **68**, also $[Y_1]^+$ at *m/z* 465. In the negative mode, both compounds presented similar ionization and fragmentation pattern: $[M-H]^-$ at

m/z 639, $[Y_1]^-$ at *m/z* 463 and $[Y_0]^-$ at *m/z* 300 (odd electron ion) and/or 301 (even electron ion).[21] Moreover, the loss of 162 *u* revealed the cleavage of a hexoxyl group, therefore these flavonols were assigned to quercetin hexose-glucuronide isomers, which had been already described in baby, romaine and iceberg lettuce cultivars,[21] but are reported here for the first time in the green and red oak-leaf cultivars.

Compounds **69** (Rt= 21.52 min, λmax= 255, 352 nm), **70** (Rt= 22.03 min, λmax= 252, 364 nm) and **71** (Rt= 23.69 min) were identified as quercetin malonylhexoside isomers since they presented $[M+H]^+$ at *m/z* 551, $[M+Na]^+$ at *m/z* 573, and $[Y_0]^+$ at *m/z* 303 due to the loss of the malonylhexoside moiety in the positive ion mode; and $[M-H]^-$at *m/z* 549, $[Y_0]^-$ at *m/z* 301, $[M-H-CO_2]^-$ at *m/z* 505 (base peak) in the negative ion mode. The neutral loss of CO_2 is characteristic of compounds presenting the malonyl group, as previously reported.[21] This fact is due to in-source fragmentation, which can affect the correct identification of the deprotonated molecule of interest, because the relative abundance of $[M-H]^-$ ion could be lower than the product ion $[M-H-CO_2]^-$ as occurred with these peaks. This particularly labile group could be partially lost during ion transfer from a higher-pressure region of the source to a lower-pressure region,[44] as observed for peak **69** (0.4 % RA), peak **70** (11 % RA) and peak **71** (0.4 % RA). The identification of compound **69** was also confirmed by the presence of $[2M-H]^-$ ion. Quercetin-3-*O*-(6''-*O*-malonyl)-glucoside has been reported in lettuce in several publications.[4, 6, 7, 9, 12, 13, 20, 39] Two isomers of quercetin malonylglucoside were already described in different lettuce varieties.[21, 38] The presence of three quercetin malonylhexoside isomers in lettuce is described for the first time in the present study.

Compound **72** (Rt= 11.51 min, λmax= 253, 355 nm) was identified as quercetin-3-*O*-(6"-*O*-malonyl)-glucoside-7-*O*-glucuronide, which has been previously described in lettuce,[4, 12, 21] however it is reported here in green oak-leaf lettuce for the first time as far as we know. In the positive ion mode, $[M+H]^+$ at *m/z* 727, $[M+Na]^+$ at *m/z* 749, and the fragment ions $[Y_1]^+$

at *m/z* 479 and $[Y_0]^+$ at *m/z* 303 indicated the loss of a malonyl-glucosyl group followed by a glucuronic group. In the negative ion mode, the neutral loss of CO_2 yielding $[M-H-CO_2]^-$ at *m/z* 681 confirmed the presence of a malonyl residue in the molecular structure; as well as the high energy function product ions at *m/z* 300 (odd electron ion) and/or 301 (even electron ion), the presence of quercetin. Similarly, compound **73** (Rt= 13.82 min, λmax= 253, 350 nm) also contained a malonyl residue since its base peak in the negative mode was $[M-H-CO_2]^-$ at *m/z* 667. The deprotonated molecule at *m/z* 711 was also present and $[Y_0]^-$ at *m/z* 300 (odd electron ion) and/or 301 (even electron ion) indicated that the aglycone was quercetin. The positive ion mode yielding $[M+H]^+$ at *m/z* 713, $[M+Na]^+$ at *m/z* 735, and the fragment ions $[Y_1]^+$ at *m/z* 465 and $[Y_0]^+$ at *m/z* 303 confirmed the cleavage of malonylhexosyl group followed by a hexosyl group. Thus, compound **73** was tentatively assigned to quercetin-3-*O*-(6"-*O*-malonyl)-glucoside-7-*O*-glucoside, which has been previously reported in lettuce [12, 21] and also in red and green oak-leaf cultivars.[4]

Compounds **74** (Rt= 12.18 min) and **75** (Rt= 16.07 min) presented the same monoisotopic molecular mass for $[M+H]^+$ at *m/z* 627.1580 ($C_{27}H_{31}O_{17}$) and $[M-H]^-$at *m/z* 625.1405 ($C_{27}H_{29}O_{17}$), and $[M+Na]^+$ at *m/z* 649.1381 ($C_{27}H_{30}O_{17}Na$). The presence of $[Y_0]^+$ at *m/z* 303 and $[Y_0]^-$ at *m/z* 301 in the positive and negative ion modes, respectively, disclosed that the aglycone was quercetin. However, these compounds followed different fragmentation patterns. Peak **74** yielded $[Y_1]^-$ at *m/z* 463 due to the loss of a hexosyl moiety (162 *u*), and revealing that $[Y_0]^-$ was obtained from the loss of a second hexosyl residue. Thus, compound **74** was assigned as a quercertin-*O*-dihexoside. Instead, peak **75** yielded $[Y_1]^-$ at *m/z* 447 due to the loss of a gluconic moiety (178 *u*), and disclosing a subsequent loss of a rhamnosyl moiety (146 *u*) to achieve $[Y_0]^-$. Peak **74** was tentatively identified as quercetin-diglucoside, which has been previously reported in green lettuce and ruby red lettuce.[12] Peak **75** was

tentatively proposed as quercertin-*O*-rhamnosylgluconide, which is here reported for the first time to the author's knowledge.

Regarding kaempferol conjugates, compound **76** (Rt= 25.27 min, λmax= 265, 347 nm) was identified as kaempferol-malonylglucoside, which has been already found in an oak-leaf cultivar.[39] In the positive mode, $[M+H]^+$ at *m/z* 535, $[M+Na]^+$ at *m/z* 557, and the fragment ions and $[Y_0]^+$ at *m/z* 287 revealed the cleavage of a malonyl-glucosyl group. In the negative mode, $[M-H]^-$at *m/z* 533, $[Y_0]^-$ at *m/z* 285, $[M-H-CO_2]^-$ at *m/z* 489 confirmed the presence of the malonyl glucosyl moiety in the molecule. Regarding the aglycone, kaempferol and the flavone luteolin are isobaric, but their conjugates can be distinguished on the basis of their MS^E data. In the positive low energy function, kaempferol derivatives yield $[Y_0]^+$ as the base peak or $[M+H]^+$ as the base peak plus an intense $[Y_0]^+$, whereas luteolin derivatives give as the base peak $[M+H]^+$ or $[M+H-H_2O]^+$, and $[Y_0]^+$ does not appear or present low relative abundance. In the negative low energy function, both compounds yield $[M-H]^-$ or $[M-H-CO_2]^-$ (in the case of malonylglycosides) as the base peak, but in the negative high energy function, kaempferol conjugates give the base peak $[Y_0]^-$, whereas luteolin compounds yield the base peak $[M-H]^-$ or $[M-H-CO_2]^-$ and an intense $[Y_0]^-$, or $[Y_0]^-$ as the base peak and an intense $[M-H]^-$ with relative abundance higher than 50% RA. Moreover, several minor monoisotopic product ions at *m/z* 217.0501 ($C_{12}H_9O_4$), 199.0395 ($C_{12}H_7O_3$), 175.0395 ($C_{10}H_7O_3$) and 133.0290 ($C_8H_5O_2$) are characteristic of luteolin, and helps to distinguish it from its kaempferol isomers.[21, 42] In this sense, these fragment ions did not appear in the negative high energy MS spectra of peak **76**, suggesting that it is a kaempferol derivative. Moreover, this identification was also supported by the base peaks yielded in the positive low energy and the negative high energy functions, $[Y_0]^+$ and $[Y_0]^-$ respectively, as well as its UV-visible spectra, and elution order since kaempferol isomers elute later than luteolin isomers on encapped C_{18} packings.

Two isomers (**77**: Rt= 23.90 min; **78**: Rt= 26.43 min) were detected in the extracted MS chromatogram at *m/z* 449 and 447 in the positive and negative ion modes respectively, which yielded the protonated molecule, $[M+Na]^+$ at *m/z* 471 and $[Y_0]^+$ at *m/z* 287 in the positive ion mode, and the deprotonated molecule and $[Y_0]^-$ at *m/z* 285 in the negative ion mode; revealing the loss of a hexosyl residue and the presence of kaempferol or luteolin aglycone. The base peaks yielded in the positive low energy and the negative high energy functions were $[Y_0]^+$ and $[Y_0]^-$ respectively, and no characteristic minor product ions of luteolin were detected in the negative high energy function, therefore the aglycone was tentatively identified as kaempferol. Compound **77** was identified unambiguously as kaempferol-3-*O*-glucoside by comparison with its standard, whereas compound **78** as kaempferol-hexoside. Kaempferol-3-*O*-glucoside is the only kaempferol-hexoside that has been previously detected in several lettuce cultivars.[15]

Compound **79** (Rt= 22.34 min, λmax= 265, 332 nm) was identified as kaempferol-3-*O*-glucuronide, which has been previously found in lettuce in literature.[11] This compound yielded $[M+H]^+$ at *m/z* 463, $[M+Na]^+$ at *m/z* 485 and $[Y_0]^+$ at *m/z* 287 in the positive mode; and $[M-H]^-$ at *m/z* 461 and $[Y_0]^-$ at *m/z* 285 in the negative mode. The observed loss of 176 *u* pointed out the presence of a glucuronic residue. Besides, the presence of the base peaks $[Y_0]^+$ and $[Y_0]^-$ in the positive low energy and the negative high energy functions respectively, and the absence of luteolin characteristic minor product ions in the negative high energy function, supports the proposed identification for this compound.

Peak **80** (Rt= 27.08 min) presented the protonated and deprotonated molecules at *m/z* 287 and 285 in the positive and the negative ion modes respectively, which yielded fragment ions which are characteristics of kaempferol or luteolin aglycones,[45] suggesting that both compounds are eluting overlapped in this peak. To the author's knowledge, kaempferol aglycone has not been previously found in lettuce, but in escarole (Asteraceae).[4]

Kaempferol-hexosides (**77** and **78**), kaempferol-3-*O*-glucuronide (**79**) and kaempferol aglycone (**80**) are reported in the green and red oak-leaf cultivars here for the first time as far as we are aware.

Flavones

Five luteolin glycosides (**81**-**85**) and five apigenin conjugates (**86**-**90**) were detected and identified on the basis of mass spectral data (Figs. 3S-4S in the supplementary information), comparing with available standards and bibliographic sources. Compound **81** (Rt= 19.82 min, λmax= 255, 347 nm) was identified unambiguously as luteolin-7-*O*-glucoside by comparison with its standard, which showed the deprotonated molecule at *m/z* 447, $[2M-H]^-$ at *m/z* 895, $[Y_0]^-$ at *m/z* 285, and luteolin characteristic minor product ions at *m/z* 217, 199 and 175 in the negative ion mode; and the protonated molecule at *m/z* 449, $[M+Na]^+$ at *m/z* 471, $[Y_0]^+$ at *m/z* 287, and intense fragment ions at 153 and 135 in the positive mode. Luteolin-7-*O*-glucoside has been previously described in lettuce cultivars.[15, 21, 38]

Compound **82** (Rt= 17.45 min, λmax= 253, 348 nm) was assigned to luteolin-7-*O*-glucuronide regarding the protonated molecule yielded at *m/z* 463, $[M+Na]^+$ at *m/z* 485 and $[Y_0]^+$ at *m/z* 287, which revealed the cleavage of a glucuronic residue (Fig. 5). In the negative high energy function, compound **82** yielded the corresponding deprotonated molecule at *m/z* 461, $[Y_0]^-$ at *m/z* 285, as well as some minor fragment ions at *m/z* 217, 199, 175, 151 and 133 (Fig. 5), which distinguished luteolin conjugates from its kaempferol isomers.[21, 42] This identification was supported by its UV-visible spectrum, which followed the luteolin pattern; and its elution order on encapped C18 packings, glucuronide conjugates elute earlier than their corresponding glucoside ones. Luteolin-7-*O*-glucuronide has been previously reported in lettuce,[12, 21, 38] and in green and red oak-leaf cultivars as well.[4, 20, 39]

Compounds **83** (Rt= 20.27 min) and **84** (Rt= 21.17 min, λmax= 268, 351 nm) showed base peaks at *m/z* 595 ($[M+H]^+$) in the low energy function. Aside, compound **84** also

presented the sodium adduct (*m/z* 617), the fragment ions at *m/z* 449 ($[Y_1]^+$), and at *m/z* 287 ($[Y_0]^+$) in the high energy function in the positive ion mode. This fragmentation pattern revealed the loss of rhamnosyl group followed by a hexosyl group, which is in agreement with the fragment ions observed in the negative ion mode, i.e. $[Y_1]^-$ at *m/z* 447 and $[Y_0]^-$ at *m/z* 285. In the negative ion mode, both compounds yielded the deprotronated molecule as the base peak in both low and high energy functions, supporting their tentatively assignment as luteolin-rhamnosylhexoside. Compound **84** was tentatively identified as luteolin-7-*O*-rutinoside since it was the major compound and has been previously found in different lettuce cultivars, including the red oak-leaf cultivar.[4] The second luteolin-rhamnosylhexoside (**83**) is here reported for the first time in lettuce to the authors' knowledge.

Compound **85** (Rt= 11.85 min, λmax= 265, 339 nm) yielded in the positive mode the protonated molecule at *m/z* 553, $[M+Na]^+$ at *m/z* 575, $[2(M-H_2O)+H]^+$ at *m/z* 1069, $[M-H_2O+H]^+$ at *m/z* 535, $[M+H-\text{hydroxymalonyl}]^+$ at *m/z* 449 and $[Y_0]^+$ at *m/z* 287; and in the negative mode, $[M-H]^-$ at *m/z* 551, $[2M-H]^-$ at *m/z* 1103, $[Y_0]^-$ at *m/z* 285, and the base peak $[M-H-CO_2]^-$ at *m/z* 507, which confirmed the presence of the malonyl moiety in the molecule. Furthermore, luteolin characteristic minor product ions at *m/z* 199 and 175 were present in the negative high energy spectrum. Therefore, compound **85** was tentatively identified as luteolin-hydroxymalonylhexoside, which has not been previously reported in lettuce in literature as far as we are aware.

Regarding apigenin derivatives, the observation of neutral losses of the conjugated groups and the product ions at *m/z* 271 and 269 in the positive and negative ion modes respectively, indicated the presence of apigenin in their structure. Thus, compound **86** (Rt= 20.57 min) showing a loss of 176 *u* was identified as apigenin-glucuronide; compound **87** (Rt= 23.02 min, λmax= 259, 328 nm) with a loss of 162 *u*, as apigenin-glucoside; and compound **88** (Rt= 23.90 min) with subsequent losses of 146 *u* and 162 *u*, as apigenin-rhamnosylhexoside, which

is here reported for the first time in lettuce cultivars. Compound **89** (Rt= 14.92 min) yielded in the positive ion mode the protonated molecule at *m/z* 465, $[M+Na]^+$ at *m/z* 487, $[Y_0]^+$ at *m/z* 271 and several minor fragments at *m/z* 163, 153, 145, 121 and 91 that contributed to confirm that the aglycone was apigenin.[23, 45] Accordingly, in the negative ion mode, it produced the deprotonated molecule at *m/z* 463 and $[Y_0]^-$ at *m/z* 269. The loss of 194.0427 *u* ($C_6H_{10}O_7$) observed was tentatively assigned to a pentahydroxyhexanoic residue. Likewise, compound **90** (Rt= 26.99 min) yielded the protonated and deprotonated molecules at *m/z* 839 and 837 and the corresponding apigenin aglycone ions in positive and negative ion modes respectively, showing a monoisotopic loss of 568.2731 *u* ($C_{25}H_{44}O_{14}$), however its identity was not able to be disclosed with the available spectral data. Apigenin-glucuronide (**86**) was detected only in the green oak-leaf variety, but not in the red cultivar. Apigenin-glucuronide (**86**) and apigenin-glucoside (**87**) have been already found in lettuce.[15, 21] Alarcón-Flores et al. (2016) found an apigenin-*O*-derivative with the same fragmentation pattern as apigenin-rhamnosylhexoside (**88**) in different lettuce cultivars, as well as luteolin aglycone (**91**, Rt= 27.08 min). However, apigenin-pentahydroxyhexanoide (**89**), only detected in the red oak-leaf cultivar, and the apigenin conjugate (**90**) have not been previously reported.

Flavanones

A flavanone glycoside was detected and identified on the basis of its UV-visible spectrum and mass spectral data. Chromatographic peak **92** (Rt= 14.87 min, λmax= 284 nm, shoulder at 329 nm) in the negative mode yielded the base peaks $[M-H]^-$ at *m/z* 463 in the low energy function, and a fragment ion $[^{1,3}A]^-$ at *m/z* 151 and an intense ion $[Y_0]^-$ at *m/z* 287 (60% RA) in the high energy function. In the positive ion mode, $[M+H]^+$ at *m/z* 465 (60% RA), $[M+Na]^+$ at *m/z* 487 and a fragment ion $[Y_0]^+$ at *m/z* 289 (base peak) were detected (Figs. 4S and 6S in the supplementary information). Both fragment ions revealed the cleavage of a glucuronic group. Moreover, minor fragments in the positive ion mode at *m/z* 153, 135 and

117 contributed to confirm that the aglycone was eriodictyol.[23] Thus, compound **92** was identified as eriodictyol-*O*-glucuronide, which is reported for the first time in lettuce to our best knowledge.

Anthocyanins

Four anthocyanins (**93**-**96**) were detected in red oak lettuce leaves, despite not working in the optimal pH conditions for their chromatographic separation (Fig. 4S in the supplementary information). Anthocyanidins are ionized much better in the positive ion mode, producing ions with higher intensities in this mode. Therefore, the ions of compounds in very low concentrations (**93** and **96**) were not detected in the negative ion mode.

Compound **93** (Rt= 10.80 min) was identified as a hexoside of cyanidin on the basis of its mass spectra with a $[M]^+$ at *m/z* 449 which yielded a high energy function fragment at *m/z* 287. The loss of 162 *u* indicated cleavage of a hexosyl residue. Its identification was confirmed by comparison with cyanidin-3-*O*-glucoside standard and bibliographic references.[46]

The MS spectra of compounds **94** (Rt= 13.62 min) and **95** (Rt= 16.84 min, λmax= 279, >500 nm) showed their base peaks $[M]^+$ at *m/z* 535 and the main product ion $[Y_0]^+$ at *m/z* 287, which corresponded to cyanidin aglycone and disclosed the loss of a malonylhexosyl residue (Fig. 6). Both compounds presented the same fragmentation pattern, but regarding the elution order for cyanidin-glycosides on non-endcapped C18 packings observed,[46] compound **94** was tentatively identified as cyanidin-3-*O*-(3''-*O*-malonyl)glucoside, and compound **95** as cyanidin-3-*O*-(6''-*O*-malonyl)-glucoside. The latter has been reported to be the most abundant anthocyanin in red leaf lettuce varieties,[9, 46] as well as observed here.

Another cyanidin glycoside eluting at 20.25 min (**96**) presented a protonated molecule at *m/z* 491 in the positive ion mode. The base peak in the low energy function was yielded at *m/z* 449, which revealed the loss of an acetyl residue; and in the high energy function, the

cyanidin aglycone ion at *m/z* 287. Regarding these observations and bibliographic data,[46] compound **96** was tentatively identified as cyanidin-3-*O*-(6''-*O*-acetyl)glucoside, which has been previously found in red leaf lettuce. Cyanidin-3-*O*-glucoside (**93**) and cyanidin-3-*O*-(6''-*O*-malonyl)glucoside (**95**) have been determined in the red oak leaf cultivar before,[9, 14, 20] however cyanidin-3-*O*-(3''-*O*-malonyl)glucoside (**94**) and cyanidin-3-*O*-(6''-*O*-acetyl)glucoside (**96**) are here reported for the first time in this red cultivar.

Coumarins

Seven coumarins (**97**-**103**) were detected in green and red oak leaf lettuce cultivars studied (Fig. 3S in the supplementary information). Chromatographic peak **97** (Rt= 6.50 min, λmax= 290, 340 nm) was identified as a 6,7-dihydroxycoumarin-6-*O*-glucoside (esculin) regarding its UV-visible spectrum and mass spectral data. In the positive ion mode, the protonated molecule at *m/z* 341, the sodium adduct at *m/z* 363 and $[Y_0]^+$ at *m/z* 179 were produced, indicating that a hexosyl group was present in the molecular structure (Fig. 7S in the supplementary information). This was confirmed in the negative ion mode, where the deprotonated molecule at *m/z* 339, the acetate adduct $[M-H+AcO]^-$ at *m/z* 399 and $[Y_0]^-$ at *m/z* 177 were yielded. Compound **97** also gave some minor fragment ions at *m/z* 133 and 105 corresponding to the loss of CO_2 and CO successively, which has been previously reported in literature,[21] and suggested that peak **97** was esculetin-6-*O*-glucoside.

Compounds **98** (Rt= 7.31 min), **99** (Rt= 10.23 min) and **100** (Rt= 12.02 min, λmax= 296, 330 nm) presented the same protonated molecule at *m/z* 179 and deprotonated molecule at *m/z* 177, as well as the same fragmentation pattern described above for esculin. Thus, they were tentatively identified as dihydrocoumarin isomers. Esculin and 6,7-dihydrocoumarin (**100**) have been already reported in lettuce and Asteraceae.[21, 47, 48] In the same way, compounds **101** (Rt= 9.05 min), **102** (Rt= 10.54 min) and **103** (Rt= 12.54 min) presented the same fragmentation patterns as the dihydrocoumarin isomers, but their protonated molecule

at *m/z* 295 and deprotonated molecule at *m/z* 293 disclosed that the loss to yield the dihydrocoumarin ion was 116 *u*, due to a maloyl residue. Thus, these compounds were tentatively assigned as maloyl-dihydrocoumarin isomers. Regarding the elution order of the dihydrocoumarin and the maloyl-dihydrocoumarin isomers, the latters are probably the maloyl derivatives of the formers, since the maloyl group increase the hydrophobicity of the molecule, and therefore, elute at higher retention times in reverse-phase packings. To the authors' knowledge, maloyl-dihydrocoumarins are reported in lettuce and Asteracea for the first time and all these coumarins are also here described for the first time in green and red oak-leaf lettuce cultivars.

Hydrolysable tannins

A tri-4-hydroxyphenylacetyl ester of a hexose (**104**, Rt= 27.09 min) was detected in the extracted trace at *m/z* 581 in the negative ion mode. This peak showed the characteristic fragmentation pattern previously described in literature,[21, 49] yielding fragment ions at *m/z* 295 ([(4-hydroxyphenylacetic acid-hexose)−H−H_2O]$^-$), *m/z* 175 ([(4-hydroxyphenylacetic acid-hexose)−2H−H_2O−$C_6H_5CH_2CO$]$^-$), *m/z* 151 ([4-hydroxyphenylacetic acid−H]$^-$ and *m/z* 143 ([(4-hydroxyphenylacetic acid-hexose)−2H−H_2O−$OHC_6H_4CH_2COOH$]$^-$ or [hexose−H−2H_2O]$^-$). Four isomers of tri-4-hydroxyphenylacetyl-glucoside were found in several *Latuca* species,[21, 49] but is here reported for the first time in green and red oak-leaf lettuce cultivars as far as we know.

Lignan derivatives

Four syringaresinol-hexoses (**105**, Rt= 13.90 min; **106**, Rt= 18.97 min; **107**, Rt= 19.63 min; **108**, Rt= 23.30 min) were detected in the extracted trace at *m/z* 579 and 581 in the negative and positive ion modes. For peak **106**, only the corresponding deprotonated and protonated molecules were detected due to its low concentration in the extract. All other isomers yielded in the negative ion mode the fragment ions corresponding to the loss of the hexose residue

(*m/z* 417), and the subsequent losses of H_2O (*m/z* 399) or two methyl residues (*m/z* 387) from the syringaresinol. In the positive ion mode, the sodium adducts (*m/z* 603) and the fragment ion due to the loss of the hexose residue plus two H_2O (*m/z* 383) were detected. In addition, three isomers of syringaresinol-acetylhexoses (**109**, Rt= 15.06 min, λmax= 205, 280 nm; **110**, Rt= 24.50 min; **111**, Rt= 24.63 min) were detected in the extracted trace at *m/z* 621 in the negative ion mode, presenting the same aforementioned fragmentation pattern (Fig. 8S in the supplementary information). In this sense, the fragment ions due to the loss of the acetylhexose residue (*m/z* 417), and the successive losses of H_2O (*m/z* 399), and methyl residues (*m/z* 402 ($-CH_3$), *m/z* 387 ($-2CH_3$)) and *m/z* 359 ($-2CH_3CO$)) were observed, as well as other further fragments from the syringaresinol structure at *m/z* 181, 166, 151 and 123.

Peaks **112** (Rt= 19.22 min), **113** (Rt= 19.39 min) and **114** (Rt= 19.82 min) were observed in the chromatogram extracted at *m/z* 581 in the negative ion mode. The MS spectra of these compounds disclosed that they presented the same fragmentation pattern as the above lignans, yielding the product ions due to the loss of the dimethoxyhexose moiety (*m/z* 359), and the subsequent losses of H_2O (*m/z* 341), and two methyl residues (*m/z* 329) from the lariciresinol structure. Thus, these compounds were proposed to be isomers of dimethoxy-hexosyl-lariciresinol. Furthermore, a dimethoxy-dihexosyl-lariciresinol isomer (**115**: Rt= 16.37 min) was also tentatively identified according to the presence of the deprotonated ion at *m/z* 743 and the fragment ion due to the loss of a hexose residue at *m/z* 581 in its negative ion MS spectra, which yielded further product ions following the same fragmentation pattern of dimethoxy-hexosyl-lariciresinol. In lettuce cultivars, only one isomer of syringaresinol-hexose (syringaresinol-β-D-glucoside) and dimethoxy-hexosyl-lariciresinol have been previously reported.[21] To the authors' knowledge, lignan derivatives are reported for the first time in oak-leaf lettuce cultivars in the present study.

Conclusions

In the present study, 109 phenolic compounds were tentatively identified in the green oak leaf lettuce cultivar, and 113 compounds in the red cultivar; of which, only 18 and 20 respectively, had been reported in these cultivars before. Previous studies had characterized up to 95 phenolics in other green lettuce varieties by UHPLC-ESI-ToF/MS and MS/MS,[8, 10, 21] and up to 24 phenolics by LC coupled to ion trap (IT) or triple quadrupole (QqQ) mass spectrometry in red varieties.[4, 9, 12, 14, 20, 46] To the authors' knowledge, the present work reports 48 phenolics not previously reported in lettuce. The UHPLC-DAD-ESI-QToF/MS^E approach demonstrates to be a useful tool for the characterization of phenolic compounds in complex plant matrices.

Acknowledgements

G.E. Viacava thanks Consejo Nacional de Investigaciones Científicas y Técnicas (CONICET) and Asociación Universitaria Iberoamericana de Postgrado (AUIP) for her Ph.D. grants. The research was supported by the Agencia Nacional de Promoción Científica y Tecnológica (project number PICT-2008-1724) and the Consejo Nacional de Investigaciones Científicas y Técnicas (CONICET) (project number PIP 0007) from Argentina.

References

[1] R.R. Watson, V.R. Preedy, S. Zibadi. *Polyphenols in human health and disease*. Academic Press, San Diego, **2014**.

[2] H.J. Heo, Y.J. Kim, D. Chung, D.-O. Kim. Antioxidant capacities of individual and combined phenolics in a model system. *Food Chem.* **2007**, *104*, 87.

[3] Z. Li, X. Zhao, A.K. Sandhu, L. Gu. Effects of exogenous abscisic acid on yield, antioxidant capacities, and phytochemical contents of greenhouse grown lettuces. *J. Agric. Food Chem.* **2010**, *58*, 6503.

[4] R. Llorach, A. Martínez-Sánchez, F.A. Tomás-Barberán, M.I. Gil, F. Ferreres. Characterisation of polyphenols and antioxidant properties of five lettuce varieties and escarole. *Food Chem.* **2008**, *108*, 1028.

[5] M.M. Oh, E.E. Carey, C.B. Rajashekar. Environmental stresses induce health-promoting phytochemicals in lettuce. *Plant Physiol. Biochem.* **2009**, *47*, 578.

[6] A. Ribas-Agustí, M. Gratacós-Cubarsí, C. Sárraga, J.A. García-Regueiro, M. Castellari. Analysis of eleven phenolic compounds including novel p-coumaroyl derivatives in lettuce (*Lactuca sativa* L.) by ultra-high-performance liquid chromatography with photodiode array and mass spectrometry detection. *Phytochem. Anal.* **2011**, *22*, 555.

[7] A. Romani, P. Pinelli, C. Galardi, G. Sani, A. Cimato, D. Heimler. Polyphenols in greenhouse and open-air-grown lettuce. *Food Chem.* **2002**, *79*, 337.

[8] A. Sofo, B. Lundegårdh, A. Mårtensson, M. Manfra, G. Pepe, E. Sommella, M. De Nisco, G.C. Tenore, P. Campiglia, A. Scopa. Different agronomic and fertilization systems affect polyphenolic profile, antioxidant capacity and mineral composition of lettuce. *Sci. Hortic.-Amsterdam* **2016**, *204*, 106.

[9] A. Marin, F. Ferreres, G.G. Barberá, M.I. Gil. Weather variability influences color and phenolic content of pigmented baby leaf lettuces throughout the season. *J. Agric. Food Chem.* **2015**, *63*, 1673.

[10] G. Pepe, E. Sommella, M. Manfra, M. De Nisco, G.C. Tenore, A. Scopa, A. Sofo, S. Marzocco, S. Adesso, T. Novellino, P. Campiglia. Evaluation of anti-inflammatory activity and fast UHPLC-DAD-IT-TOF profiling of polyphenolic compounds extracted from green lettuce (*Lactuca sativa* L.; Var. Maravilla de Verano). *Food Chem.* **2015**, *167*, 153.

[11] S.W. Jeong, G.-S. Kim, W.S. Lee, Y.-H. Kim, N.J. Kang, J.S. Jin, G.M. Lee, S.T. Kim, A.M. Abd El-Aty, J.-H. Shim, S.C. Shin. The effects of different night-time

temperatures and cultivation durations on the polyphenolic contents of lettuce: Application of principal component analysis. *J. Adv. Res.* **2015**, *6*, 493.

[12] J. Santos, M.B.P.P. Oliveira, E. Ibáñez, M. Herrero. Phenolic profile evolution of different ready-to-eat baby-leaf vegetables during storage. *J. Chromatogr. A* **2014**, *1327*, 118.

[13] F. Mai, M.A. Glomb. Isolation of phenolic compounds from iceberg lettuce and impact on enzymatic browning. *J. Agric. Food Chem.* **2013**, *61*, 2868.

[14] C. Becker, H.P. Klaering, L.W. Kroh, A. Krumbein. Cool-cultivated red leaf lettuce accumulates cyanidin-3-O-(6″-O-malonyl)-glucoside and caffeoylmalic acid. *Food Chem.* **2014**, *146*, 404.

[15] M.I. Alarcón-Flores, R. Romero-González, J.L. Martínez Vidal, A. Garrido Frenich. Multiclass determination of phenolic compounds in different varieties of tomato and lettuce by ultra high performance liquid chromatography coupled to tandem mass spectrometry. *Int. J. Food Prop.* **2016**, *19*, 494.

[16] R. Jaiswal, J. Kiprotich, N. Kuhnert. Determination of the hydroxycinnamate profile of 12 members of the Asteraceae family. *Phytochemistry* **2011**, *72*, 781.

[17] A. Altunkaya, V. Gökmen. Effect of various anti-browning agents on phenolic compounds profile of fresh lettuce (L. sativa). *Food Chem.* **2009**, *117*, 122.

[18] A.P. Sobolev, E. Brosio, R. Gianferri, A.L. Segre. Metabolic profile of lettuce leaves by high-field NMR spectra. *Magn. Reson. Chem.* **2005**, *43*, 625.

[19] U. Złotek, M. Świeca, A. Jakubczyk. Effect of abiotic elicitation on main health-promoting compounds, antioxidant activity and commercial quality of butter lettuce (*Lactuca sativa* L.). *Food Chem.* **2014**, *148*, 253.

[20] C. Becker, H.P. Klaering, M. Schreiner, L.W. Kroh, A. Krumbein. Unlike quercetin glycosides, cyanidin glycoside in red leaf lettuce responds more sensitively to increasing low

radiation intensity before than after head formation has started. *J. Agric. Food Chem.* **2014**, *62*, 6911.

[21] I.M. Abu-Reidah, M.M. Contreras, D. Arráez-Román, A. Segura-Carretero, A. Fernández-Gutiérrez. Reversed-phase ultra-high-performance liquid chromatography coupled to electrospray ionization-quadrupole-time-of-flight mass spectrometry as a powerful tool for metabolic profiling of vegetables: *Lactuca sativa* as an example of its application. *J. Chromatogr. A* **2013**, *1313*, 212.

[22] M. Ramirez-Ambrosi, B. Abad-Garcia, M. Viloria-Bernal, S. Garmon-Lobato, L.A. Berrueta, B. Gallo. A new ultrahigh performance liquid chromatography with diode array detection coupled to electrospray ionization and quadrupole time-of-flight mass spectrometry analytical strategy for fast analysis and improved characterization of phenolic compounds in apple products. *J. Chromatogr. A* **2013**, *1316*, 78.

[23] B. Abad-García, L.A. Berrueta, S. Garmón-Lobato, B. Gallo, F. Vicente. A general analytical strategy for the characterization of phenolic compounds in fruit juices by high-performance liquid chromatography with diode array detection coupled to electrospray ionization and triple quadrupole mass spectrometry. *J. Chromatogr. A* **2009**, *1216*, 5398.

[24] K.R. Markham. *Techniques of Flavonoid Identification*. AcademicPress Inc., London, **1982**.

[25] Y.L. Ma, Q.M. Li, H. Van den Heuvel, M. Claeys. Characterization of flavone and flavonol aglycones by collision-induced dissociation tandem mass spectrometry. *Rapid Commun. Mass Spectrom.* **1997**, *11*, 1357.

[26] N. Lozac'h. Nomenclature of Cyclitols. *Eur. J. Biochem.* **1975**, *57*, 1.

[27] M. Gómez-Romero, A. Segura-Carretero, A. Fernandez-Gutierrez. Metabolite profiling and quantification of phenolic compounds in methanol extracts of tomato fruit. *Phytochemistry* **2010**, *71*, 1848.

[28] R.M. Alonso-Salces, C. Guillou, L.A. Berrueta. Liquid chromatography coupled with ultraviolet absorbance detection, electrospray ionization, collision-induced dissociation and tandem mass spectrometry on a triple quadrupole for the on-line characterization of polyphenols and methylxanthines in green coffee beans. *Rapid Commun. Mass Spectrom.* **2009**, *23*, 363.

[29] M.N. Clifford, K.L. Johnston, S. Knight, N. Kuhnert. Hierarchical scheme for LC-MS^n identification of chlorogenic acids. *J. Agric. Food Chem.* **2003**, *51*, 2900.

[30] M.N. Clifford, S. Knight, B. Surucu, N. Kuhnert. Characterization by LC-MS^n of four new classes of chlorogenic acids in green coffee beans: Dimethoxycinnamoylquinic acids, diferuloylquinic acids, caffeoyl-dimethoxycinnamoylquinic acids, and feruloyl-dimethoxycinnamoylquinic acids. *J. Agric. Food Chem.* **2006**, *54*, 1957.

[31] M.N. Clifford, S. Knight, N. Kuhnert. Discriminating between the six isomers of dicaffeoylquinic acid by LC-MS^n. *J. Agric. Food Chem.* **2005**, *53*, 3821.

[32] M.N. Clifford. in, (Eds: C. Santos-Buelga, G. Williamson), Royal Society of Chemistry, Cambridge, **2003**, pp. 314.

[33] M.N. Clifford, W. Wu, J. Kirkpatrick, N. Kuhnert. Profiling the chlorogenic acids and other caffeic acid derivatives of herbal chrysanthemum by LC-MS^n. *J. Agric. Food Chem.* **2007**, *55*, 929.

[34] M.N. Clifford, J. Kirkpatrick, N. Kuhnert, H. Roozendaal, P.R. Salgado. LC-MS^n analysis of the cis isomers of chlorogenic acids. *Food Chem.* **2008**, *106*, 379.

[35] M.N. Clifford, W. Wu, N. Kuhnert. The chlorogenic acids of Hemerocallis. *Food Chem.* **2006**, *95*, 574.

[36] B. Möller, K. Herrmann. Analysis of quinic acid esters of hydroxycinnamic acids in plant material by capillary gas chromatography and high-performance liquid chromatography. *J. Chromatogr. A* **1982**, *241*, 371.

[37] A.L. Dawidowicz, R. Typek. The influence of pH on the thermal stability of 5-*O*-caffeoylquinic acids in aqueous solutions. *Eur. Food Res. Technol.* **2011**, *233*, 223.

[38] L.Z. Lin, J. Harnly, R.W. Zhang, X.E. Fan, H.J. Chen. Quantitation of the hydroxycinnamic acid derivatives and the glycosides of flavonols and flavones by UV absorbance after identification by LC-MS. *J. Agric. Food Chem.* **2012**, *60*, 544.

[39] D. Heimler, L. Isolani, P. Vignolini, S. Tombelli, A. Romani. Polyphenol content and antioxidative activity in some species of freshly consumed salads. *J. Agric. Food Chem.* **2007**, *55*, 1724.

[40] F.A. Tomás-Barberán, J. Loaiza-Velarde, A. Bonfanti, M.E. Saltveit. Early wound- and ethylene-induced changes in phenylpropanoid metabolism in harvested lettuce. *J. Am. Soc. Hort. Sci.* **1997**, *122*, 399.

[41] M.N. Clifford, S. Marks, S. Knight, N. Kuhnert. Characterization by LC-MS^n of four new classes of p-coumaric acid-containing diacyl chlorogenic acids in green coffee beans. *J. Agric. Food Chem.* **2006**, *54*, 4095.

[42] M. Gómez-Romero, G. Zurek, B. Schneider, C. Baessmann, A. Segura-Carretero, A. Fernández-Gutiérrez. Automated identification of phenolics in plant-derived foods by using library search approach. *Food Chem.* **2011**, *124*, 379.

[43] I.M. Abu-Reidah, D. Arráez-Román, R. Quirantes-Piné, S. Fernández-Arroyo, A. Segura-Carretero, A. Fernández-Gutiérrez. HPLC–ESI-Q-TOF-MS for a comprehensive characterization of bioactive phenolic compounds in cucumber whole fruit extract. *Food Res. Int.* **2012**, *46*, 108.

[44] V. Katta, S.K. Chowdhury, B.T. Chait. Use of a single-quadrupole mass spectrometer for collision-induced dissociation studies of multiply charged peptide ions produced by electrospray ionization. *Anal. Chem.* **1991**, *63*, 174.

[45] B. Abad-García, Búsqueda de marcadores químicos de tipo polifenólico para la autentificación de zumos de frutas, in, Universidad del País Vasco/Euskal Herriko Unibertsitatea (UPV/EHU), Bilbao, Spain, 2007, pp. 865.

[46] X. Wu, R.L. Prior. Identification and characterization of anthocyanins by high-performance liquid chromatography-electrospray ionization-tandem mass spectrometry in common foods in the United States: Vegetables, nuts, and grains. *J. Agric. Food Chem.* **2005**, *53*, 3101.

[47] S. Rees, J. Harborne. Flavonoids and other phenolics of Cichorium and related members of the Lactuceae (Compositae). *Bot. J. Linn. Soc.* **1984**, *89*, 313.

[48] K. Schütz, R. Carle, A. Schieber. Taraxacum–A review on its phytochemical and pharmacological profile. *J. Ethnopharmacol.* **2006**, *107*, 313.

[49] R.A. Sessa, M.H. Bennett, M.J. Lewis, J.W. Mansfield, M.H. Beale. Metabolite profiling of sesquiterpene lactones from Lactuca species. Major latex components are novel oxalate and sulfate conjugates of lactucin and its derivatives. *J. Biol. Chem.* **2000**, *275*, 26877.

Figure captions

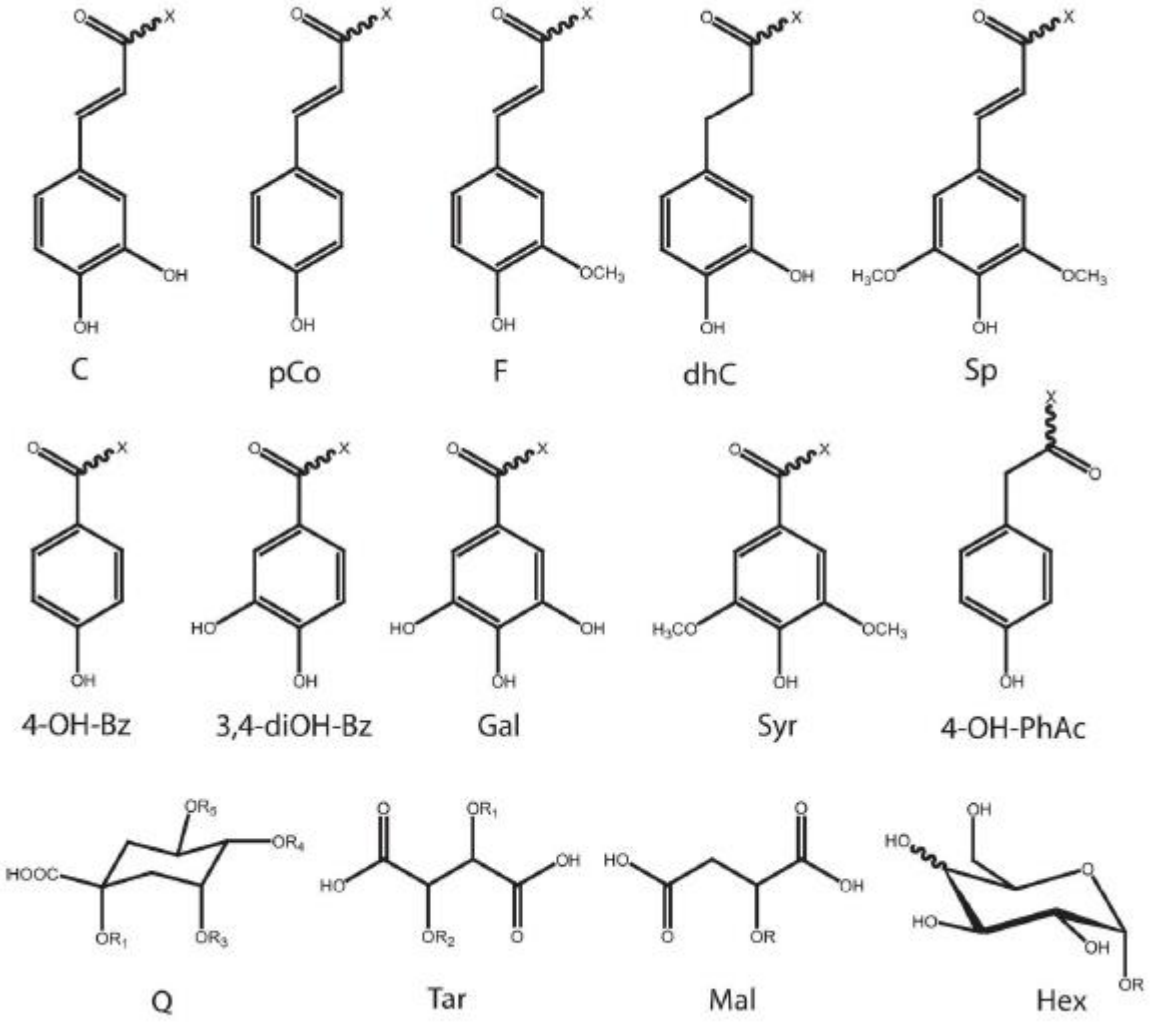

Figure 1. Chemical structures of phenolic acids and their derivatives found in oak leaf lettuce cultivars. Abbreviations for the phenolic moieties: C, caffeoyl; pCo, p-coumaroyl; F, feruloyl; dhC, dihydrocaffeoyl; Sp, sinapoyl; 4-OH-Bz, 4-hydroxybenzoyl; 3,4-diOH-Bz, 3,4-dihydroxybenzoyl; Gal, galloyl; Syr, syringoyl; 4-OH-PhAc, 4-hydroxyphenylacetoyl. Abbreviations for the non-phenolic moieties: Q, quinic acid; Tar, tartaric acid, Mal, malic acid; Mln, malonic acid; Glcr, glucuronic acid; Glcn, gluconic acid; Hex, hexose; Rha, rhamnose;

Rut, rutinose (rhamnosylglucose). R, R_1, R_2, R_3, R_4 and R_5 can be esterified in position X of phenolic acids (X=H) or etherified with phenolic OH groups.

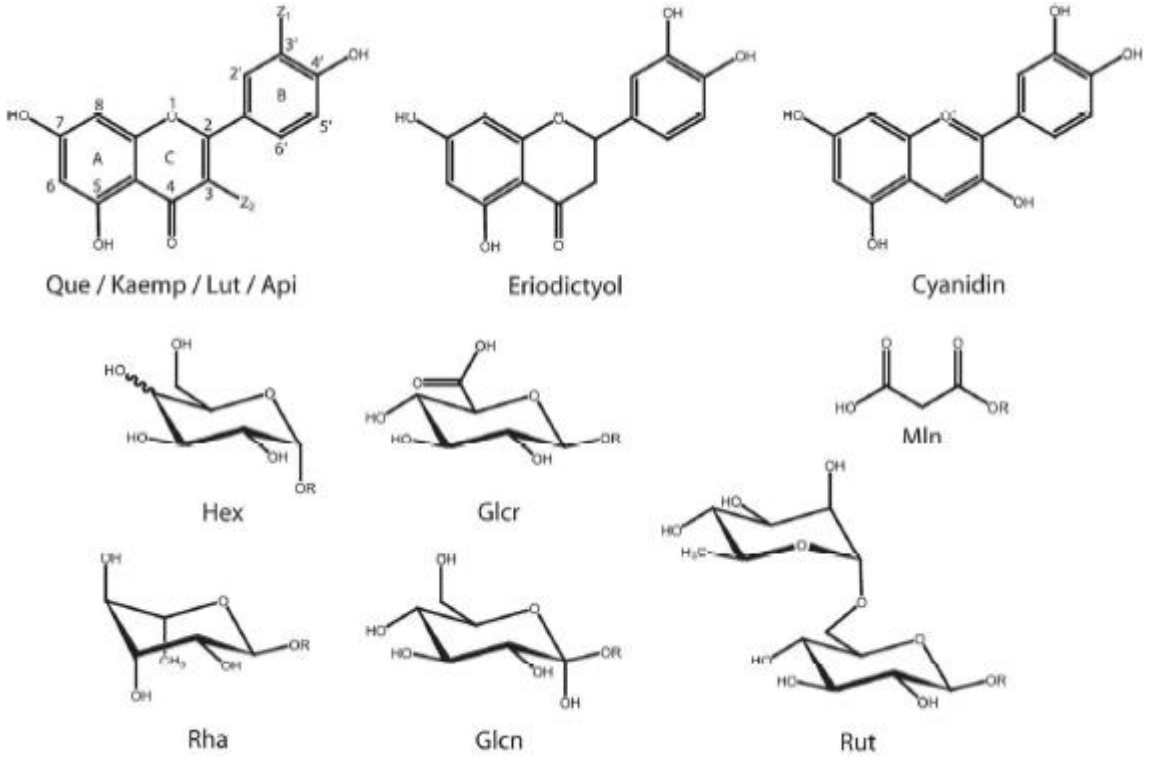

Figure 2. Chemical structures of flavonoids found in oak leaf lettuce cultivars. Abbreviations for phenolic moieties: Que, quercetin (Z_1=OH, Z_2=OH); Kaemp, kaempferol (Z_1=H, Z_2=OH); Lut, luteolin (Z_1=OH, Z_2=H); Api, apigenin (Z_1=H, Z_2=H). Abbreviations for the non-phenolic moieties: Glcr, glucuronic acid; Glcn, gluconic acid; Hex, hexose; Rha, rhamnose; Rut, rutinose (rhamnosylglucose). Non-phenolic moieties can be etherified with phenolic OH groups.

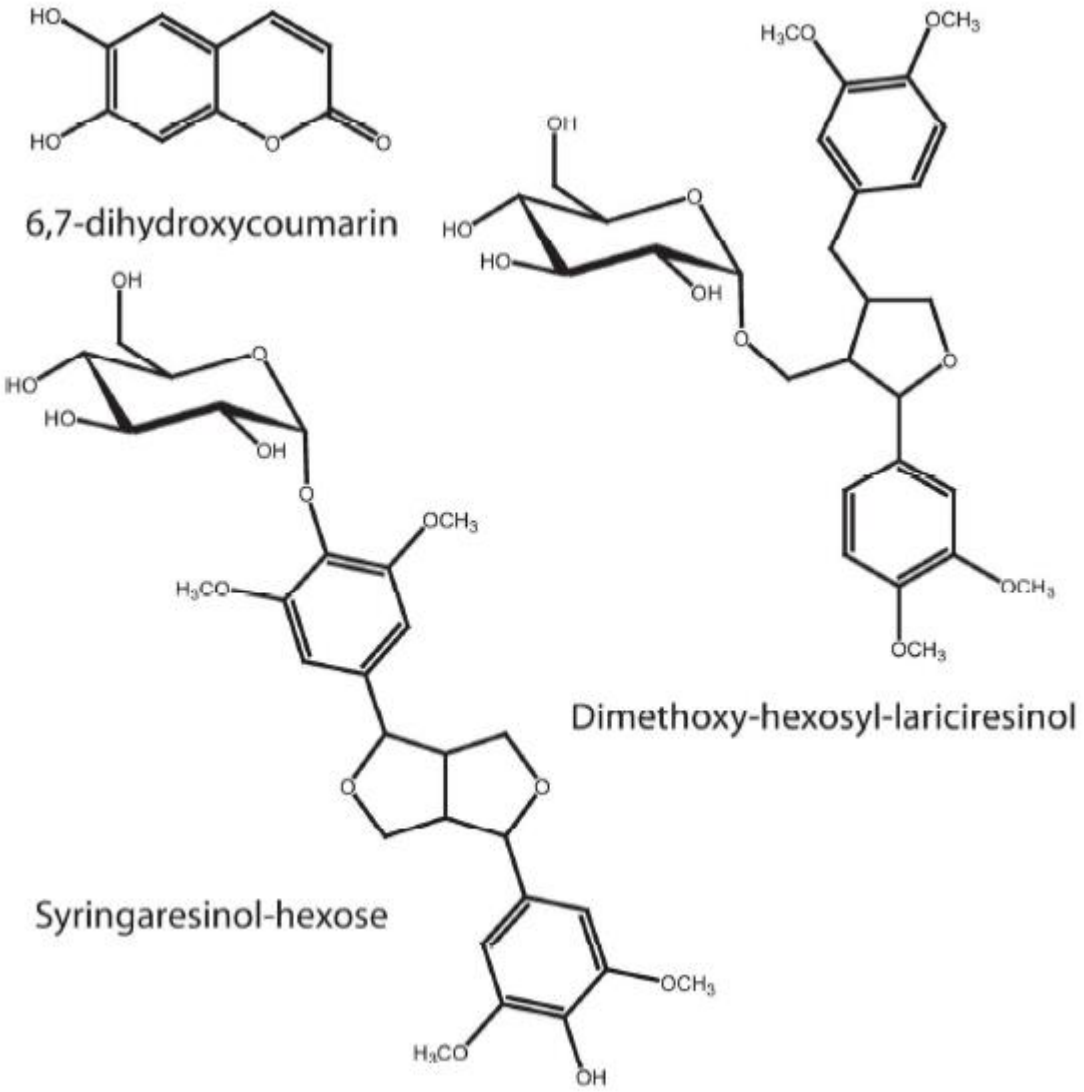

Figure 3. Chemical structures of coumarins and lignan derivatives found in oak leaf lettuce cultivars.

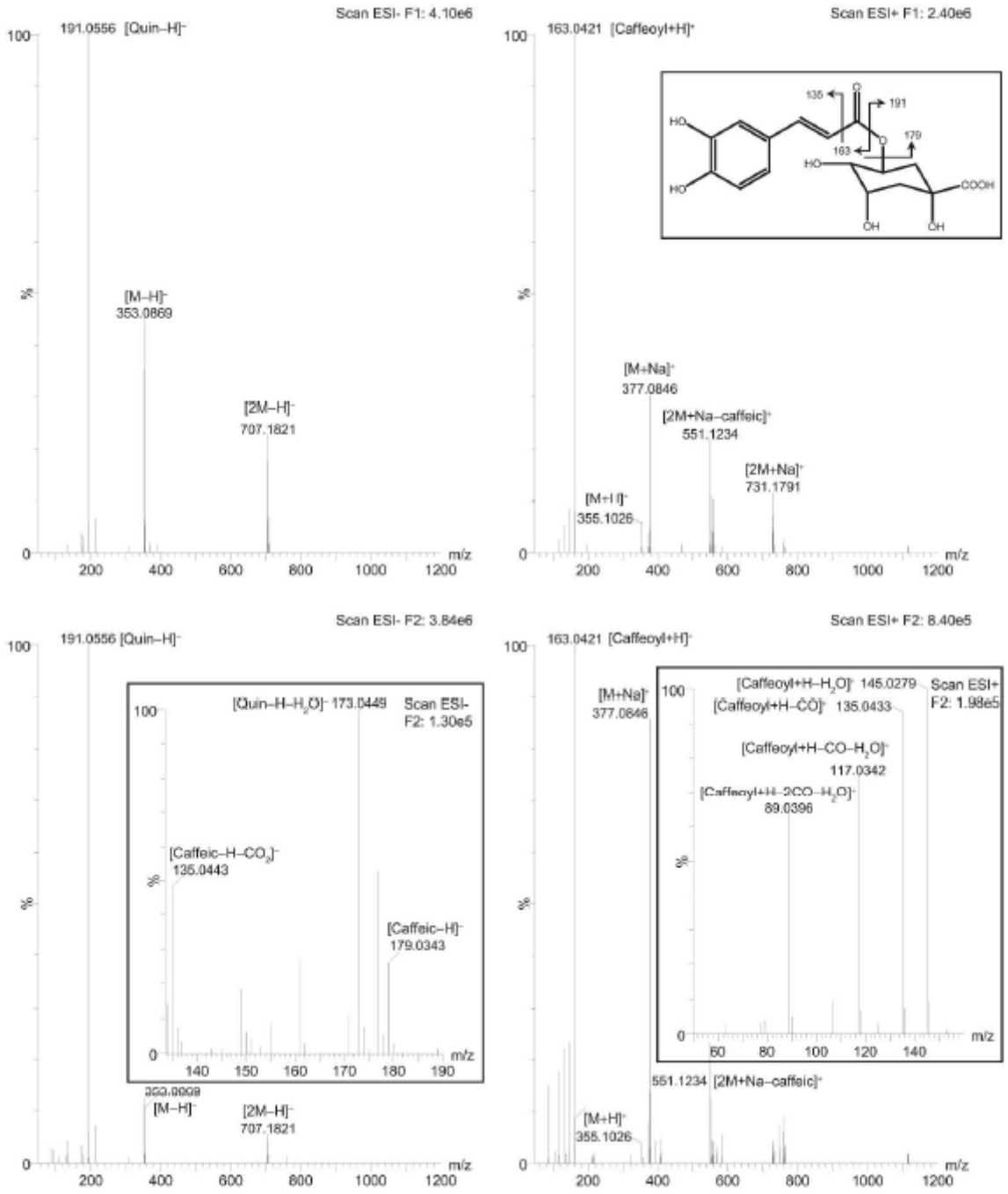

Figure 4. Low (F1) and high (F2) energy function MS spectra in the negative and positive ion mode of 5-*trans*-*O*-caffeoylquinic acid.

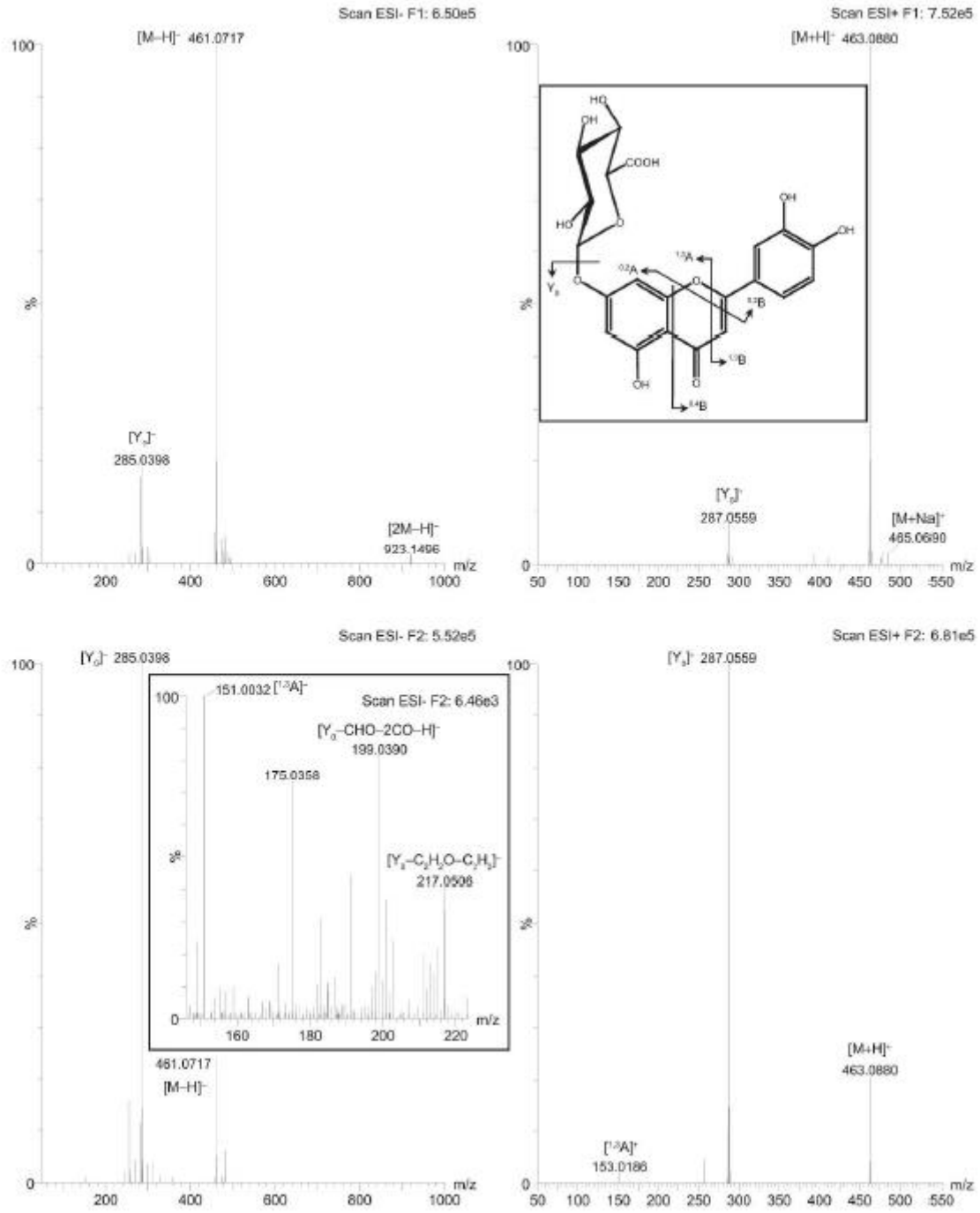

Figure 5. Low (F1) and high (F2) energy function MS spectra in the negative and positive ion mode of luteolin-7-*O*-glucuronide.

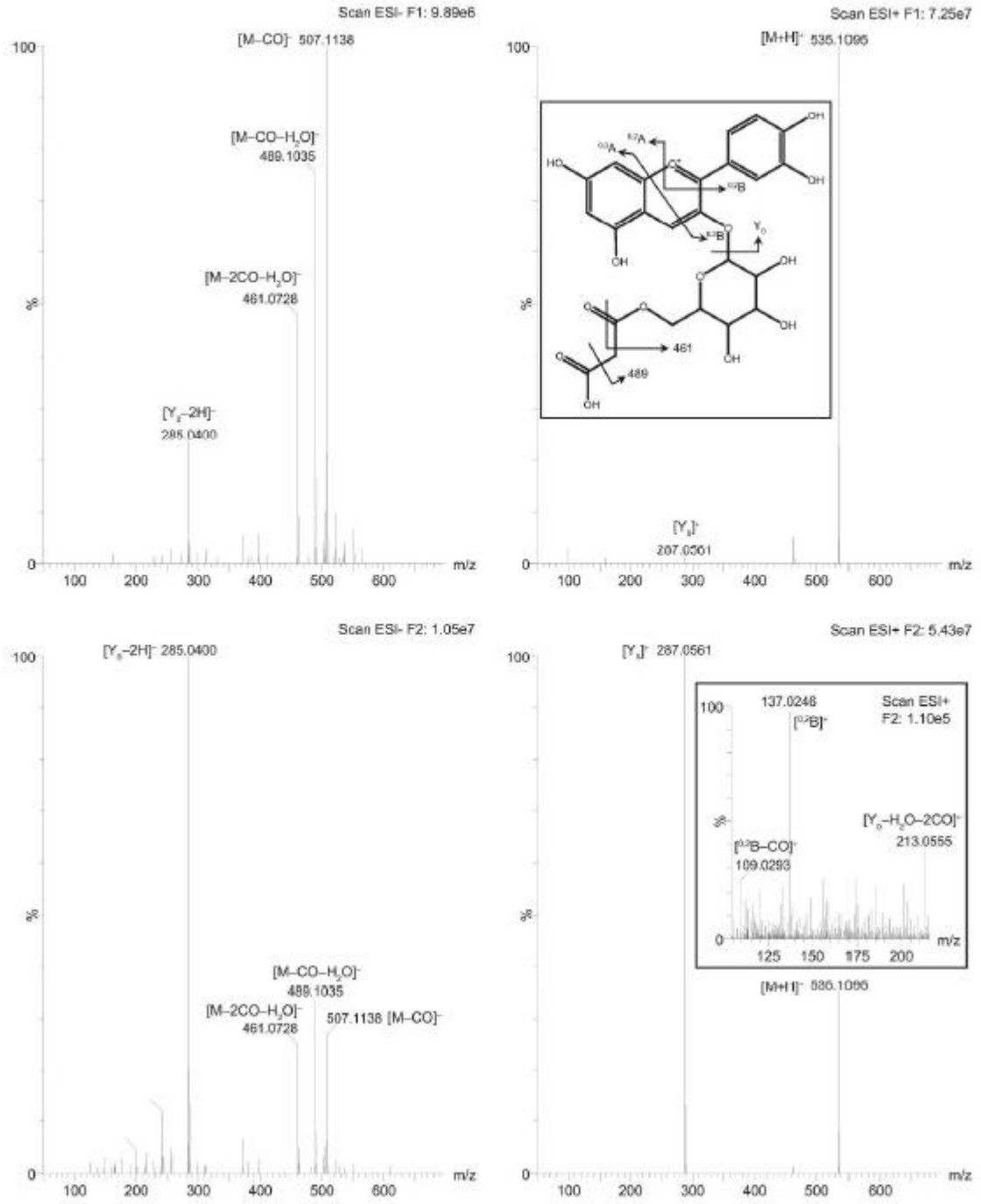

Figure 6. Low (F1) and high (F2) energy function MS spectra in the negative and positive ion mode of cyaniding-3-*O*-(6″-*O*-malonyl)-glucoside.

Tables

Table 1. Retention times, UV-visible maxima and MS^E data of phenolic acids identified by UHPLC-DAD-ESI-Q-ToF/MS in oak leaf lettuce cultivars.[a,b,c]

	LC	DAD	ESI(+)–QToF/MS					ESI(–)–QToF/MS					Assignment
Nº	Rt (min)	UV bands (nm)	Exp. Acc. Mass $[M+H]^+$	Error (mDa)	Formula $[M+H]^+$	Adducts & fragment ions of $[M+H]^+$ *m/z*		Exp. Acc. Mass $[M-H]^-$	Error (mDa)	Formula $[M-H]^-$	Adducts & fragment ions of $[M-H]^-$ *m/z*		Tentative identification
	Hydroxycinnamic derivatives												
	Caffeoylquinic acids												
1	4.74	301 sh, 323	355.1068	3.9	$C_{16}H_{19}O_9$	377.0858	$[M+Na]^+$	353.0872	–0.1	$C_{16}H_{17}O_9$	191.0556	$[Quin-H]^-$ *(100)*	3–*trans*–*O*–Caffeoylquinic acid
						163.0398	$[Caffeoyl+H]^+$				179.0348	$[Caffeic-H]^-$ *(32)*	
						145.0279	$[Caffeoyl+H-H_2O]^+$				173.0437	$[Quin-H-H_2O]^-$ *(4)*	
						135.0448	$[Caffeoyl+H-CO]^+$				135.0446	$[Caffeic-H-CO_2]^-$ *(71)*	
						117.0343	$[Caffeoyl+H-CO-H_2O]^+$						
						89.0397	$[Caffeoyl+H-H_2O-2CO]^+$						
2	6.65	-	355.1026	–0.3	$C_{16}H_{19}O_9$	731.1791	$[2M+Na]^+$	353.0869	0.4	$C_{16}H_{17}O_9$	707.1821	$[2M-H]^-$	1–*trans*–*O*–Caffeoylquinic acid
						551.1234	$[2M+Na-caffeic]^+$				191.0561	$[Quin-H]^-$ *(100)*	
						377.0846	$[M+Na]^+$						
						163.0421	$[Caffeoyl+H]^+$						
						145.0279	$[Caffeoyl+H-H_2O]^+$						
						135.0433	$[Caffeoyl+H-CO]^+$						
						117.0342	$[Caffeoyl+H-CO-H_2O]^+$						
						89.0396	$[Caffeoyl+H-H_2O-2CO]^+$						
3	7.32	300 sh, 324	355.1026	–0.3	$C_{16}H_{19}O_9$	731.1791	$[2M+Na]^+$	353.0869	–0.4	$C_{16}H_{17}O_9$	707.1821	$[2M-H]^-$	5–*trans*–*O*–Caffeoylquinic acid
						551.1234	$[2M+Na-caffeic]^+$				191.0556	$[Quin-H]^-$ *(100)*	
						377.0846	$[M+Na]^+$				179.0343	$[Caffeic-H]^-$ *(1)*	
						163.0421	$[Caffeoyl+H]^+$				173.0449	$[Quin-H-H_2O]^-$ *(3)*	
						145.0279	$[Caffeoyl+H-H_2O]^+$				135.0443	$[Caffeic-H-CO_2]^-$ *(2)*	
						135.0433	$[Caffeoyl+H-CO]^+$						
						117.0342	$[Caffeoyl+H-CO-H_2O]^+$						
						89.0396	$[Caffeoyl+H-H_2O-2CO]^+$						
4	8.12	–	355.1068	3.9	$C_{16}H_{19}O_9$	731.1739	$[2M+Na]^+$	353.0861	–1.2	$C_{16}H_{17}O_9$	707.1796	$[2M-H]^-$	3–*cis*–*O*–Caffeoylquinic acid
						709.1981	$[2M+H]^+$				191.0557	$[Quin-H]^-$ *(100)*	
						163.0397	$[Caffeoyl+H]^+$				179.0344	$[Caffeic-H]^-$ *(12)*	
						145.0128	$[Caffeoyl+H-H_2O]^+$				135.0441	$[Caffeic-H-CO_2]^-$ *(21)*	
						135.0463	$[Caffeoyl+H-CO]^+$						
						117.0333	$[Caffeoyl+H-CO-H_2O]^+$						
						89.0383	$[Caffeoyl+H-H_2O-2CO]^+$						
5	8.36	–	355.1068	3.9	$C_{16}H_{19}O_9$	377.0844	$[M+Na]^+$	353.0865	–0.8	$C_{16}H_{17}O_9$	191.0554	$[Quin-H]^-$ *(100)*	4–*trans*–*O*–Caffeoylquinic acid
						163.0445	$[Caffeoyl+H]^+$				173.0458	$[Quin-H-H_2O]^-$ *(13)*	
						145.0325	$[Caffeoyl+H-H_2O]^+$						
						135.0408	$[Caffeoyl+H-CO]^+$						
						117.0364	$[Caffeoyl+H-CO-H_2O]^+$						
6	10.23	301 sh, 316	355.1068	3.9	$C_{16}H_{19}O_9$	731.1746	$[2M+Na]^+$	353.0867	–0.6	$C_{16}H_{17}O_9$	707.1816	$[2M-H]^-$	5–*cis*–*O*–Caffeoylquinic acid
						551.1199	$[2M+Na-caffeic]^+$				191.0557	$[Quin-H]^-$ *(100)*	
						377.0841	$[M+Na]^+$				173.0449	$[Quin-H-H_2O]^-$ *(3)*	
						163.0400	$[Caffeoyl+H]^+$						
						145.0284	$[Caffeoyl+H-H_2O]^+$						

Nº	LC	DAD	ESI(+)–QToF/MS					ESI(–)–QToF/MS					Assignment
	Rt (min)	UV bands (nm)	Exp. Acc. Mass $[M+H]^+$	Error (mDa)	Formula $[M+H]^+$	Adducts & fragment ions of $[M+H]^+$ *m/z*		Exp. Acc. Mass $[M-H]^-$	Error (mDa)	Formula $[M-H]^-$	Adducts & fragment ions of $[M-H]^-$ *m/z*		Tentative identification
						135.0443	[Caffeoyl+H–CO]$^+$						
						117.0346	[Caffeoyl+H–CO–H_2O]$^+$						
						89.0396	[Caffeoyl+H–H_2O–2CO]$^+$						
7	15.06	–			$C_{16}H_{19}O_9$	163.0399	[Caffeoyl+H]$^+$	353.0876	0.3	$C_{16}H_{17}O_9$	191.0578	[Quin–H]$^-$ *(100)*	4–*cis*–*O*–Caffeoylquinic acid
						145.0287	[Caffeoyl+H–H_2O]$^+$				179.0314	[Caffeic–H]$^-$ *(5)*	
						135.0446	[Caffeoyl+H–CO]$^+$				173.0455	[Quin–H–H_2O]$^-$ *(2)*	
						117.0278	[Caffeoyl+H–CO–H_2O]$^+$						
	p-Coumaroylquinic acids												
8	9.82	312	339.1075	–0.5	$C_{16}H_{19}O_8$	699.1888	[2M+Na]$^+$	337.0921	–0.2	$C_{16}H_{17}O_8$	675.1904	[2M–H]$^-$	3–*p*–Coumaroylquinic acid
						361.0892	[M+Na]$^+$				191.0467	[Quin–H]$^-$	
						147.0451	[*p*Coumaroyl+H]$^+$				163.0393	[*p*Coumaric–H]$^-$	
						119.0500	[*p*Coumaroyl+H–CO]$^+$				119.0496	[*p*Coumaric–H–CO_2]$^-$	
						91.0556	[*p*Coumaroyl+H–2CO]$^+$						
9	13.74	308	339.1133	5.3	$C_{16}H_{19}O_8$	699.1916	[2M+Na]$^+$	337.0919	–0.4	$C_{16}H_{17}O_8$	191.0553	[Quin–H]$^-$	5–*p*–Coumaroylquinic acid
						361.0907	[M+Na]$^+$				173.0449	[Quin–H–H_2O]$^-$	
						147.0453	[*p*Coumaroyl+H–H_2O]$^+$				163.0390	[*p*Coumaric–H]$^-$	
						119.0500	[*p*Coumaroyl+H–H_2O–CO]$^+$				119.0491	[*p*Coumaric–H–CO_2]$^-$	
						91.0561	[*p*Coumaroyl+H–H_2O–2CO]$^+$						
	Caffeoyltartaric acid												
10	9.06	301 sh, 323			$C_{13}H_{13}O_9$			311.0526	–12.3	$C_{13}H_{11}O_9$	293.0287	[Caftar–H–H_2O]$^-$	Caffeoyltartaric acid
											179.0349	[Caffeic–H]$^-$	
											149.0227	[Tartaric–H]$^-$	
											135.0432	[Caffeic–H–CO_2]$^-$	
	p-Coumaroyltartaric acid												
11	15.63	310			$C_{13}H_{13}O_8$			295.0457	–0.3	$C_{13}H_{11}O_8$	163.0393	[*p*Coumaric–H]$^-$	*p*–Coumaroyltartaric acid
											149.0104	[Tartaric–H]$^-$	
											119.0481	[*p*Coumaric–H–CO_2]$^-$	
	Caffeoylmalic acid												
12	9.05	301 sh, 323	297.0585	–2.5	$C_{13}H_{13}O_8$	319.0429	[M+Na]$^+$	295.0448	–0.6	$C_{13}H_{11}O_8$	591.0983	[2M–H]$^-$	Caffeoylmalic acid
						163.0404	[Caffeoyl+H]$^+$				179.0345	[Caffeic–H]$^-$	
						145.0297	[Caffeoyl+H–H_2O]$^+$				135.0446	[Caffeic–H–CO_2]$^-$	
						135.0447	[Caffeoyl+H–CO]$^+$				133.0275	[Malic–H]$^-$	
						117.0348	[Caffeoyl+H–CO–H_2O]$^+$				115.0032	[Malic–H–H_2O]$^-$	
						89.0397	[Caffeoyl+H–H_2O–2CO]$^+$				105.0342	[Malic–H–CO]$^-$	
	Dicaffeoylquinic acids and caffeoylquinic acid glycosides												
13	5.86	–	517.1548	0.9	$C_{22}H_{29}O_{14}$	539.1364	[M+Na]$^+$	515.1402	0.1	$C_{22}H_{27}O_{14}$	353.0869	[Cafquin–H]$^-$	Caffeoylquinic acid–hexoside
						355.1038	[M–hexosyl]$^+$				191.0548	[Quin–H]$^-$	
						163.0415	[Caffeoyl+H]$^+$						
						145.0310	[Caffeoyl+H–H_2O]$^+$						
						135.0449	[Caffeoyl+H–CO]$^+$						
						117.0385	[Caffeoyl+H–CO–H_2O]$^+$						
						89.0399	[Caffeoyl+H–H_2O–2CO]$^+$						
14	7.56	–			$C_{22}H_{29}O_{14}$	539.1367	[M+Na]$^+$	515.1402	0.1	$C_{22}H_{27}O_{14}$			Caffeoylquinic acid–hexoside
15	20.20	321	517.1423	7.7	$C_{25}H_{25}O_{12}$	539.1155	[M+Na]$^+$	515.1194	0.4	$C_{25}H_{23}O_{12}$	353.0871	[Cafquin–H]$^-$	1,5–di–*O*–Caffeoylquinic acid
						499.1237	[M+H–H_2O]$^+$				335.0771	[Cafquin–H–H_2O]$^-$	
						355.0985	[Cafquin+H]$^+$				191.0558	[Quin–H]$^-$	

	LC	DAD	ESI(+)–QToF/MS					ESI(–)–QToF/MS					Assignment
Nº	Rt (min)	UV bands (nm)	Exp. Acc. Mass $[M+H]^+$	Error (mDa)	Formula $[M+H]^+$	Adducts & fragment ions of $[M+H]^+$ *m/z*		Exp. Acc. Mass $[M-H]^-$	Error (mDa)	Formula $[M-H]^-$	Adducts & fragment ions of $[M-H]^-$ *m/z*		Tentative identification
						163.0403	[Caffeoyl+H]$^+$				179.0349	[Caffeic–H]$^-$	
						145.0159	[Caffeoyl+H–H_2O]$^+$				135.0448	[Caffeic–H–CO_2]$^-$	
						135.0451	[Caffeoyl+H–CO]$^+$						
						117.0350	[Caffeoyl+H–CO–H_2O]$^+$						
						89.0404	[Caffeoyl+H–H_2O–2CO]$^+$						
16	20.63	326	517.1332	–1.4	$C_{25}H_{25}O_{12}$	539.1155	[M+Na]$^+$	515.1186	–0.4	$C_{25}H_{23}O_{12}$	353.0866	[Cafquin–H]$^-$	3,5–di–*O*–Caffeoylquinic acid
						499.1230	[M+H–H_2O]$^+$				335.0761	[Cafquin–H–H_2O]$^-$	
						355.1016	[Cafquin+H]$^+$				191.0556	[Quin–H]$^-$	
						163.0401	[Caffeoyl+H]$^+$				179.0347	[Caffeic–H]$^-$	
						145.0291	[Caffeoyl+H–H_2O]$^+$				135.0446	[Caffeic–H–CO_2]$^-$	
						135.0450	[Caffeoyl+H–CO]$^+$						
						117.0346	[Caffeoyl+H–CO–H_2O]$^+$						
						89.0401	[Caffeoyl+H–H_2O–2CO]$^+$						
17	24.17	331	517.1423	7.7	$C_{25}H_{25}O_{12}$	539.1165	[M+Na]$^+$	515.1190	0.0	$C_{25}H_{23}O_{12}$	353.0860	[Cafquin–H]$^-$	4,5–di–*O*–Caffeoylquinic acid
						499.1228	[M+H–H_2O]$^+$				335.0802	[Cafquin–H–H_2O]$^-$	
						473.2006	[M+H–CO_2]$^+$				179.0347	[Caffeic–H]$^-$	
						355.0161	[Cafquin+H]$^+$				173.0449	[Quin–H–H_2O]$^-$	
						163.0395	[Caffeoyl+H]$^+$				135.0441	[Caffeic–H–CO_2]$^-$	
						135.0447	[Caffeoyl+H–CO]$^+$						
						117.0347	[Caffeoyl+H–CO–H_2O]$^+$						
						89.0400	[Caffeoyl+H–H_2O–2CO]$^+$						
	p-Coumaroylcaffeoylquinic acids												
18	23.58	312	501.1384	1.3	$C_{25}H_{25}O_{11}$	523.1219	[M+Na]$^+$	499.1233	0.7	$C_{25}H_{23}O_{11}$	353.0868	[M–H–coumaroyl]$^-$	3–*p*–Coumaroyl–4–caffeoylquinic acid
						483.1295	[M+H–H_2O]$^+$				337.0916	[M–H–caffeoyl]$^-$	
						163.0399	[Caffeoyl+H–H_2O]$^+$				191.0560	[Quin–H]$^-$	
						147.0446	[*p*Coumaroyl+H]$^+$				179.0353	[Caffeic–H]$^-$	
						145.0279	[Caffeoyl+H–2H_2O]$^+$				163.0398	[*p*Coumaric–H]$^-$	
						135.0455	[Caffeoyl+H–H_2O–CO]$^+$				135.0452	[Caffeic–H–CO_2]$^-$	
						119.0497	[*p*Coumaroyl+H–H_2O–CO]$^+$				119.0503	[*p*Coumaric–H–CO_2]$^-$	
						117.0335	[Caffeoyl+H–2H_2O–CO]$^+$						
						91.0550	[*p*Coumaroyl+H–H_2O–2CO]$^+$						
						89.0398	[Caffeoyl+H–2H_2O–2CO]$^+$						
19	23.95	316	501.1377	2.0	$C_{25}H_{25}O_{11}$	523.1216	[M+Na]$^+$	499.1241	–0.1	$C_{25}H_{23}O_{11}$	353.0852	[M–H–coumaroyl]$^-$	4–Caffeoyl–5–*p*–coumaroylquinic acid
						483.1281	[M+H–H_2O]$^+$				337.0928	[M–H–caffeoyl]$^-$	
						147.0445	[*p*Coumaroyl+H]$^+$				191.0553	[Quin–H]$^-$	
						119.0493	[*p*Coumaroyl+H–CO]$^+$				179.0342	[Caffeic–H]$^-$	
						91.0550	[*p*Coumaroyl+H–2CO]$^+$				163.0390	[*p*Coumaric–H]$^-$	
											135.0448	[Caffeic–H–CO_2]$^-$	
											119.0490	[*p*Coumaric–H–CO_2]$^-$	
	Dicaffeoyltartaric acids												
20	10.53	301 sh, 324			$C_{22}H_{19}O_{12}$	497.0677	[M+Na]$^+$	473.0719	–0.1	$C_{22}H_{17}O_{12}$	947.1354	[2M–H]$^-$	di–*O*–Caffeoyltartaric acid
						457.0698	[M+H–H_2O]$^+$				311.0402	[Caftar–H]$^-$	
						295.0577	[Caftar–H–H_2O]$^+$				293.0296	[Caftar–H–H_2O]$^-$	
						163.0397	[Caffeoyl+H]$^+$				179.0345	[Caffeic–H]$^-$	
						145.0292	[Caffeoyl+H–H_2O]$^+$				149.0091	[Tartaric–H]$^-$	
						135.0448	[Caffeoyl+H–CO]$^+$				135.0443	[Caffeic–H–CO_2]$^-$	
						117.0343	[Caffeoyl+H–CO–H_2O]$^+$				105.0339	[Tartaric–H–CO_2]$^-$	
						89.0396	[Caffeoyl+H–H_2O–2CO]$^+$						

	LC	DAD	ESI(+)–QToF/MS					ESI(–)–QToF/MS					Assignment
Nº	**Rt (min)**	**UV bands (nm)**	**Exp. Acc. Mass $[M+H]^+$**	**Error (mDa)**	**Formula $[M+H]^+$**	**Adducts & fragment ions of $[M+H]^+$** *m/z*		**Exp. Acc. Mass $[M-H]^-$**	**Error (mDa)**	**Formula $[M-H]^-$**	**Adducts & fragment ions of $[M-H]^-$** *m/z*		**Tentative identification**
21	12.54	301 sh, 323			$C_{22}H_{19}O_{12}$	295.0563	$[Caftar-H-H_2O]^+$	473.0713	–0.7	$C_{22}H_{17}O_{12}$	311.0387	$[Caftar-H]^-$	*meso*–di–*O*–Caffeoyltartaric acid
						163.0398	$[Caffeoyl+H]^+$				293.0297	$[Caftar-H-H_2O]^-$	
						145.0288	$[Caffeoyl+H-H_2O]^+$				179.0346	$[Caffeic-H]^-$	
						135.0446	$[Caffeoyl+H-CO]^+$				149.0126	$[Tartaric-H]^-$	
						117.0341	$[Caffeoyl+H-CO-H_2O]^+$				135.0448	$[Caffeic-H-CO_2]^-$	
						89.0398	$[Caffeoyl+H-H_2O-2CO]^+$				105.0343	$[Tartaric-H-CO_2]^-$	
	Other hydroxycinnamic acids												
22	5.39	–	343.1098	6.9	$C_{15}H_{19}O_9$	365.0878	$[M+Na]^+$	341.0905	–3.2	$C_{15}H_{17}O_9$			Caffeic acid–hexoside
						163.0394	$[Caffeoyl+H]^+$						
						145.0104	$[Caffeoyl+H-H_2O]^+$						
						135.0497	$[Caffeoyl+H-CO]^+$						
						89.0401	$[Caffeoyl+H-H_2O-2CO]^+$						
23	5.64	–			$C_{15}H_{19}O_9$	365.0833	$[M+Na]^+$	341.0854	1.9	$C_{15}H_{17}O_9$	179.0330	$[Caffeic-H]^-$	Caffeic acid–hexoside
						163.0389	$[Caffeoyl+H]^+$				135.0435	$[Caffeic-H-CO_2]^-$	
						145.0289	$[Caffeoyl+H-H_2O]^+$						
						135.0473	$[Caffeoyl+H-CO]^+$						
						117.0309	$[Caffeoyl+H-CO-H_2O]^+$						
24	6.08	301 sh, 325			$C_{15}H_{19}O_9$	365.0844	$[M+Na]^+$	341.0873	0.0	$C_{15}H_{17}O_9$	179.0348	$[Caffeic-H]^-$	Caffeic acid–hexoside
											135.0452	$[Caffeic-H-CO_2]^-$	
25	7.69	–			$C_{15}H_{19}O_9$	365.0843	$[M+Na]^+$	341.0876	–0.3	$C_{15}H_{17}O_9$	179.0351	$[Caffeic-H]^-$	Caffeic acid–hexoside
											135.0449	$[Caffeic-H-CO_2]^-$	
26	8.44	–			$C_{15}H_{19}O_9$	365.0855	$[M+Na]^+$	341.0867	0.6	$C_{15}H_{17}O_9$	179.0349	$[Caffeic-H]^-$	Caffeic acid–hexoside
						163.0405	$[Caffeoyl+H]^+$				135.0432	$[Caffeic-H-CO_2]^-$	
						145.0137	$[Caffeoyl+H-H_2O]^+$						
						135.0455	$[Caffeoyl+H-CO]^+$						
						117.0343	$[Caffeoyl+H-CO-H_2O]^+$						
						89.0383	$[Caffeoyl+H-H_2O-2CO]^+$						
27	9.01	–			$C_{15}H_{19}O_9$			341.0897	–2.4	$C_{15}H_{17}O_9$	179.0349	$[Caffeic-H]^-$	Caffeic acid–hexoside
											135.0432	$[Caffeic-H-CO_2]^-$	
28	9.52	–			$C_{15}H_{19}O_9$	365.0837	$[M+Na]^+$	341.0883	–1.0	$C_{15}H_{17}O_9$	179.0355	$[Caffeic-H]^-$	Caffeic acid–hexoside
						145.0078	$[Caffeoyl+H-H_2O]^+$				135.0448	$[Caffeic-H-CO_2]^-$	
						135.0471	$[Caffeoyl+H-CO]^+$						
						117.0334	$[Caffeoyl+H-CO-H_2O]^+$						
						89.0275	$[Caffeoyl+H-H_2O-2CO]^+$						
29	9.64	–			$C_{15}H_{19}O_9$	163.0380	$[Caffeoyl+H]^+$	341.0897	–2.4	$C_{15}H_{17}O_9$	135.0442	$[Caffeic-H-CO_2]^-$	Caffeic acid–hexoside
						145.0338	$[Caffeoyl+H-H_2O]^+$						
						135.0482	$[Caffeoyl+H-CO]^+$						
						117.0348	$[Caffeoyl+H-CO-H_2O]^+$						
						89.0275	$[Caffeoyl+H-H_2O-2CO]^+$						
30	8.01	301 sh, 325	359.0802	3.5	$C_{18}H_{15}O_8$	163.0415	$[Caffeoyl+H]^+$	357.0633	–2.3	$C_{18}H_{13}O_8$			Caffeoyl–derivative
						145.0640	$[Caffeoyl+H-H_2O]^+$						
						135.0390	$[Caffeoyl+H-CO]^+$						
						117.0346	$[Caffeoyl+H-CO-H_2O]^+$						
						89.0407	$[Caffeoyl+H-H_2O-2CO]^+$						
31	6.03	301 sh, 326			$C_{17}H_{23}O_{10}$	409.1092	$[M+Na]^+$	385.1138	–0.3	$C_{17}H_{21}O_{10}$	208.0659	$[M-H-hexosyl-CH_3]^-$	Sinapic acid–hexoside
						225.0745	$[M+H-hexosyl]^+$				179.0350	$[M-H-hexosyl-CO_2]^-$	
											164.0519	$[M-H-hexosyl-CH_3-CO_2]^-$	
											149.0620	$[M-H-hexosyl-2CH_3-CO_2]^-$	

	LC	DAD	ESI(+)–QToF/MS					ESI(–)–QToF/MS					Assignment
Nº	Rt (min)	UV bands (nm)	Exp. Acc. Mass $[M+H]^+$	Error (mDa)	Formula $[M+H]^+$	Adducts & fragment ions of $[M+H]^+$ *m/z*		Exp. Acc. Mass $[M-H]^-$	Error (mDa)	Formula $[M-H]^-$	Adducts & fragment ions of $[M-H]^-$ *m/z*		Tentative identification
32	9.70	–			$C_{17}H_{23}O_{10}$	409.0938	$[M+Na]^+$	385.1117	1.8	$C_{17}H_{21}O_{10}$	223.0605	$[M-H-hexosyl]^-$	Sinapic acid–hexoside
						225.0774	$[M+H-hexosyl]^+$				208.0372	$[M-H-hexosyl-CH_3]^-$	
						207.0665	$[M+H-hexosyl-H_2O]^+$				179.0725	$[M-H-hexosyl-CO_2]^-$	
						192.0411	$[M+H-hexosyl-H-CH_3OH]^+$				164.0486	$[M-H-hexosyl-CH_3-CO_2]^-$	
						175.0411	$[M+H-hexosyl-H_2O-CH_3OH]^+$				149.0222	$[M-H-hexosyl-2CH_3-CO_2]^-$	
						129.0381	$[M+H-hexosyl-2H_2O-CO-CH_3OH]^+$						
33	10.36	–			$C_{17}H_{23}O_{10}$	409.1115	$[M+Na]^+$	385.1124	1.1	$C_{17}H_{21}O_{10}$			Sinapic acid–hexoside
						192.0430	$[M+H-hexosyl-H-CH_3OH]^+$						
34	13.13	–			$C_{17}H_{23}O_{10}$	409.1111	$[M+Na]^+$	385.1112	2.3	$C_{17}H_{21}O_{10}$	223.0598	$[M-H-hexosyl]^-$	Sinapic acid–hexoside
						225.0753	$[M+H-hexosyl]^+$				208.0365	$[M-H-hexosyl-CH_3]^-$	
						207.0620	$[M+H-hexosyl-H_2O]^+$				179.0576	$[M-H-hexosyl-CO_2]^-$	
						192.0416	$[M+H-hexosyl-H-CH_3OH]^+$				164.0473	$[M-H-hexosyl-CH_3-CO_2]^-$	
						175.0461	$[M+H-hexosyl-H_2O-CH_3OH]^+$				149.0234	$[M-H-hexosyl-2CH_3-CO_2]^-$	
						129.0322	$[M+H-hexosyl-2H_2O-CO-CH_3OH]^+$						
35	8.32	–			$C_{15}H_{19}O_8$	349.0901	$[M+Na]^+$	325.0914	0.9	$C_{15}H_{17}O_8$	163.0397	$[M-H-hexosyl]^-$	*p*–Coumaric acid–hexoside
						147.0449	$[pCoumaroyl+H-H_2O]^+$				119.0493	$[M-H-hexosyl-CO_2]^-$	
						119.0506	$[pCoumaroyl+H-H_2O-CO]^+$						
						91.0569	$[pCoumaroyl+H-H_2O-2CO]^+$						
36	3.70	–			$C_{15}H_{21}O_9$			343.1029	0.0	$C_{15}H_{19}O_9$	181.0496	$[DihydroCaf-H]^-$	Dihydrocaffeic acid–hexoside
						367.0989	$[M+Na]^+$				163.0393	$[DihydroCaf-H-H_2O]^-$	
											135.0450	$[DihydroCaf-H-H_2O-CO]^-$	
											119.0489	$[DihydroCaf-H-H_2O-CO_2]^-$	
37	3.83	–			$C_{15}H_{21}O_9$			343.1028	0.1	$C_{15}H_{19}O_9$	181.0504	$[DihydroCaf-H]^-$	Dihydrocaffeic acid–hexoside
						367.0999	$[M+Na]^+$				163.0398	$[DihydroCaf-H-H_2O]^-$	
											135.0450	$[DihydroCaf-H-H_2O-CO]^-$	
											119.0492	$[DihydroCaf-H-H_2O-CO_2]^-$	
38	11.81	307			$C_{11}H_{13}O_4$			207.0650	0.7	$C_{11}H_{11}O_4$	192.0422	$[M-H-CH_3]^-$	Ferulic acid methyl ester
39	14.47	–			$C_{11}H_{13}O_4$			207.0663	–0.6	$C_{11}H_{11}O_4$	192.0422	$[M-H-CH_3]^-$	Ferulic acid methyl ester
											177.0206	$[M-H-2CH_3]^-$	
											133.0685	$[M-H-CH_3-CO_2]^-$	
40	16.48	–			$C_{11}H_{13}O_4$			207.0656	0.1	$C_{11}H_{11}O_4$	192.0435	$[M-H-CH_3]^-$	Ferulic acid methyl ester
											177.0206	$[M-H-2CH_3]^-$	
											133.0686	$[M-H-CH_3-CO_2]^-$	
	Hydroxybenzoic acid derivatives												
41	4.67	–		3.6	$C_7H_6O_4$	138.0281	$[M]^+$	137.0238	0.1	$C_7H_5O_3$	109.0294	$[M-H-CO]^-$	Hydroxybenzoic acid
											93.0331	$[M-H-CO_2]^-$	
42	5.42	–			$C_7H_7O_4$			153.0196	–0.8	$C_7H_5O_4$	135.0448	$[DiHBZ-H-H_2O]^-$	Dihydroxybenzoic acid
											109.0294	$[M-H-CO_2]^-$	
43	4.22	–			$C_{13}H_{17}O_8$			299.0733	3.4	$C_{13}H_{15}O_8$	271.0141	$[M-H-CO]^-$	Hydroxybenzoic acid–hexoside
											137.0216	$[HBZ-H]^-$	
											93.0498	$[HBZ-H-CO_2]^-$	
44	5.15	–			$C_{13}H_{17}O_8$			299.0764	0.3	$C_{13}H_{15}O_8$	137.0244	$[HBZ-H]^-$	Hydroxybenzoic acid–hexoside
45	2.49	–			$C_{13}H_{17}O_9$			315.0714	0.2	$C_{13}H_{15}O_9$	153.0181	$[DiHBZ-H]^-$	Dihydroxybenzoic acid–hexoside
											152.0114	$[DiHBZ-2H]^-$	
											135.0441	$[DiHBZ-H-H_2O]^-$	
											109.0283	$[DiHBZ-H-CO_2]^-$	
46	2.69	–			$C_{13}H_{17}O_9$			315.0714	0.2	$C_{13}H_{15}O_9$	153.0181	$[DiHBZ-H]^-$	Dihydroxybenzoic acid–hexoside
											152.0114	$[DiHBZ-2H]^-$	

Nº	LC	DAD	ESI(+)–QToF/MS					ESI(–)–QToF/MS					Assignment
	Rt (min)	UV bands (nm)	Exp. Acc. Mass $[M+H]^+$	Error (mDa)	Formula $[M+H]^+$	Adducts & fragment ions of $[M+H]^+$ *m/z*		Exp. Acc. Mass $[M-H]^-$	Error (mDa)	Formula $[M-H]^-$	Adducts & fragment ions of $[M-H]^-$ *m/z*		Tentative identification
											135.0441	$[DiHBZ-H-H_2O]^-$	
											109.0283	$[DiHBZ-H-CO_2]^-$	
47	3.74	–			$C_{13}H_{17}O_9$			315.0716	0.0	$C_{13}H_{15}O_9$	153.0185	$[DiHBZ-H]^-$	Dihydroxybenzoic acid–hexoside
											109.0287	$[DiHBZ-H-CO_2]^-$	
48	3.91	–			$C_{13}H_{17}O_9$			315.0716	0.0	$C_{13}H_{15}O_9$	153.0172	$[DiHBZ-H]^-$	Dihydroxybenzoic acid–hexoside
											109.0307	$[DiHBZ-H-CO_2]^-$	
49	4.48	–			$C_{13}H_{17}O_9$			315.0716	0.0	$C_{13}H_{15}O_9$	153.0172	$[DiHBZ-H]^-$	Dihydroxybenzoic acid–hexoside
											152.0108	$[DiHBZ-2H]^-$	
											135.0441	$[DiHBZ-H-H_2O]^-$	
											109.0261	$[DiHBZ-H-CO_2]^-$	
50	4.68	–			$C_{13}H_{17}O_9$			315.0717	–0.1	$C_{13}H_{15}O_9$	153.0196	$[DiHBZ-H]^-$	Dihydroxybenzoic acid–hexoside
											135.0442	$[DiHBZ-H-H_2O]^-$	
											109.0298	$[DiHBZ-H-CO_2]^-$	
51	2.80	–						331.0661	–0.4	$C_{13}H_{15}O_{10}$	313.0557	$[M-H-H_2O]^-$	Gallic acid–hexoside
											169.0113	$[Gallic-H]^-$	
											168.0057	$[Gallic-2H]^-$	
											149.9953	$[Gallic-2H-H_2O]^-$	
											125.0226	$[Gallic-H-CO_2]^-$	
52	2.88	–						331.0661	–0.4	$C_{13}H_{15}O_{10}$	313.0557	$[M-H-H_2O]^-$	Gallic acid–hexoside
											169.0113	$[Gallic-H]^-$	
											168.0057	$[Gallic-2H]^-$	
											149.9953	$[Gallic-2H-H_2O]^-$	
											125.0226	$[Gallic-H-CO_2]^-$	
53	6.61	–						331.0660	0.5	$C_{13}H_{15}O_{10}$	313.0544	$[M-H-H_2O]^-$	Gallic acid–hexoside
											169.0140	$[Gallic-H]^-$	
											168.0054	$[Gallic-2H]^-$	
											149.9953	$[Gallic-2H-H_2O]^-$	
											125.0232	$[Gallic-H-CO_2]^-$	
54	5.90	–	361.1107	2.8	$C_{15}H_{21}O_{10}$	97.0288	$[M+H-glucosyl-2CH_3-CO-CO_2]^+$	359.0975	0.3	$C_{15}H_{19}O_{10}$	197.0454	$[M-H-glucosyl]^-$	Syringic acid–hexoside
											182.0210	$[M-H-glucosyl-CH_3]^-$	
											153.0561	$[M-H-glucosyl-CO_2]^-$	
											138.0337	$[M-H-glucosyl-CH_3-CO_2]^-$	
											123.0105	$[M-H-glucosyl-2CH_3-CO_2]^-$	
55	17.09	–			$C_{20}H_{21}O_{12}$			451.0880	–0.3	$C_{20}H_{19}O_{12}$	331.0682	$[M-H]^-$	Hydroxybenzoyl gallic acid–hexoside
											313.0558	$[M-H-H_2O]^-$	
											168.0060	$[Gallic-2H]^-$	
											124.0160	$[Gallic-2H-CO_2]^-$	
56	24.83	–			$C_{20}H_{21}O_{12}$			451.0865	1.2	$C_{20}H_{19}O_{12}$	331.0660	$[M-H]^-$	Hydroxybenzoyl gallic acid–hexoside
											313.0544	$[M-H-H_2O]^-$	
											168.0054	$[Gallic-2H]^-$	
											124.0163	$[Gallic-2H-CO_2]^-$	
57	17.68	–			$C_{20}H_{21}O_{11}$			435.0933	–0.6	$C_{20}H_{19}O_{11}$	315.0722	$[DiHBZhex-H]^-$ or $[M-OC_6H_4CO]^-$	Hydroxybenzoyl–*O*–dihydroxybenzoic acid–hexoside
											153.0184	$[DiHBZ-H]^-$	
											152.0126	$[DiHBZ-2H]^-$	
											137.0258	$[HBZ-H]^-$	
											108.0227	$[DiHBZ-2H-CO_2]^-$	
											93.0344	$[HBZ-H-CO_2]^-$	
58	19.41	–			$C_{20}H_{21}O_{11}$			435.0927	0.0	$C_{20}H_{19}O_{11}$	315.0710	$[DiHBZhex-H]^-$ or $[M-OC_6H_4CO]^-$	Hydroxybenzoyl–*O*–dihydroxybenzoic

	LC	DAD	ESI(+)–QToF/MS				ESI(–)–QToF/MS					Assignment
Nº	Rt (min)	UV bands (nm)	Exp. Acc. Mass $[M+H]^+$	Error (mDa)	Formula $[M+H]^+$	Adducts & fragment ions of $[M+H]^+$ *m/z*	Exp. Acc. Mass $[M–H]^–$	Error (mDa)	Formula $[M–H]^–$	Adducts & fragment ions of $[M–H]^–$ *m/z*		Tentative identification
												acid–hexoside
										153.0192	$[DiHBZ–H]^–$	
										108.0189	$[DiHBZ–2H–CO_2]^–$	
59	23.64	–			$C_{20}H_{21}O_{11}$		435.0920	0.7	$C_{20}H_{19}O_{11}$			Hydroxybenzoyl–*O*–dihydroxybenzoic acid–hexoside
60	26.88	256,			$C_{20}H_{21}O_{11}$		435.0925	0.2	$C_{20}H_{19}O_{11}$	315.0471	$[DiHBZhex–H]^–$ or $[M–OC_6H_4CO]^–$	Hydroxybenzoyl–*O*–dihydroxybenzoic acid–hexoside
		335 sh								297.0611	$[DiHBZhex–H–H_2O]^–$	
										152.0117	$[DiHBZ–2H]^–$	
										137.0238	$[HBZ–H]^–$	
										108.0215	$[DiHBZ–2H–CO_2]^–$	
										93.0337	$[HBZ–H–CO_2]^–$	
61	27.09	–			$C_{20}H_{21}O_{11}$		435.0927	0.0	$C_{20}H_{19}O_{11}$	315.0715	$[DiHBZhex–H]^–$ or $[M–OC_6H_4CO]^–$	Hydroxybenzoyl–*O*–dihydroxybenzoic acid–hexoside
										297.0609	$[DiHBZhex–H–H_2O]^–$	
										153.0195	$[DiHBZ–H]^–$	
										137.0240	$[HBZ–H]^–$	
										108.0215	$[DiHBZ–2H–CO_2]^–$	
										93.0341	$[HBZ–H–CO_2]^–$	
	Hydroxyphenylacetic derivatives											
62	5.60	–			$C_8H_9O_3$		151.0392	0.3	$C_8H_7O_3$	123.0439	$[M–H–CO]^–$	4–hydroxyphenylacetic acid
										107.0500	$[M–H–CO_2]^–$	

[a] Fragment ions produced in MS were named according to Ma et al. (1997).

[b] Abbreviations: Caffeic, caffeic acid; Cafquin, caffeoylquinic acid; Caftar, caffeoyltartaric acid; DiHBZ, dihydroxybenzoic acid; DiHBZhex, dihydroxybenzoic acid-hexoside; DihydroCaf, dihydrocaffeic acid; Gallic, gallic acid; HBZ, hydroxybenzoic acid; hex, hexose; 4-hydroxyphenylacetic, 4-hydroxyphenylacetic acid; 4-hydroxyphenylacetichex, 4-hydroxyphenylacetic acid-hexoside ; Malic, malic acid; pCoumaric, *p*-coumaric acid; Quin, quinic acid; Tartaric, tartaric acid; sh, shoulder.

[c] Abundances of the fragment ions of caffeoylquinic acids in the negative mode are given in parenthesis.

Table 2. Retention times, UV-visible maxima and MS^E data of flavonoids identified by UHPLC-DAD-ESI-Q-ToF/MS in oak leaf lettuce cultivars.[a]

	LC	DAD	ESI(+)–QToF/MS					ESI(–)–QToF/MS					Assignment
Nº	Rt (min)	UV bands (nm)	Exp. Acc. Mass $[M+H]^+$	Error (mDa)	Formula $[M+H]^+$	Adducts & fragment ions of $[M+H]^+$ *m/z*		Exp. Acc. Mass $[M-H]^-$	Error (mDa)	Formula $[M-H]^-$	Adducts & fragment ions of $[M-H]^-$ *m/z*		Tentative identification
Flavonols													
63	17.16	279, 344	465.1022	–1.1	$C_{21}H_{21}O_{12}$	487.0832	$[M+Na]^+$	463.0874	–0.3	$C_{21}H_{19}O_{12}$	301.0341	$[Y_0]^-$	Quercetin–*O*–hexoside
						303.0501	$[Y_0]^+$				255.0237	$[Y_0–CHO–OH]^-$	
						145.0090	$[Y_0–CHO–OH–4CO]^+$				227.0332	$[Y_0–2CO–H_2O]^-$	
											151.0027	$[^{1,3}A]^-$	
											133.0685	$[^{1,3}B–H_2O]^-$	
64	18.03	252, 367	465.1007	–2.6	$C_{21}H_{21}O_{12}$	487.0834	$[M+Na]^+$	463.0888	1.1	$C_{21}H_{19}O_{12}$	301.0356	$[Y_0]^-$	Quercetin–*O*–hexoside
						303.0465	$[Y_0]^+$				255.0310	$[Y_0–CHO–OH]^-$	
						229.0492	$[Y_0–CHO–OH–CO]^+$				151.0037	$[^{1,3}A]^-$	
						153.0186	$[^{1,3}A]^+$				107.0137	$[^{0,2}A–2CO]^{-};[^{0,2}B–CO]^-$	
65	20.25	252, 330	465.1032	–0.1	$C_{21}H_{21}O_{12}$	487.0840	$[M+Na]^+$	463.0880	0.3	$C_{21}H_{19}O_{12}$	301.0339	$[Y_0]^-$	Quercetin 3–*O*–galactoside
						303.0504	$[Y_0]^+$				255.0303	$[Y_0–CHO–OH]^-$	
						229.0492	$[Y_0–CHO–OH–CO]^+$				151.0039	$[^{1,3}A]^-$	
66	18.44	254, 349	479.0826	0.0	$C_{21}H_{19}O_{13}$	501.0644	$[M+Na]^+$	477.0675	1.1	$C_{21}H_{17}O_{13}$	301.0347	$[Y_0]^-$	Quercetin–3–*O*–glucuronide
						303.0507	$[Y_0]^+$				299.0200	$[Y_0–2H]^-$	
						257.0443	$[Y_0–CHO–OH]^+$				255.0293	$[Y_0–CHO–OH]^-$	
						153.0186	$[^{1,3}A]^+$				227.0346	$[Y_0–2CO–H_2O]^-$	
											151.0036	$[^{1,3}A]^-$	
67	9.50	256, 352	641.1385	3.1	$C_{27}H_{29}O_{18}$	663.1232	$[M+Na]^+$	639.1168	–2.9	$C_{27}H_{27}O_{18}$	463.0865	$[Y_1]^-$	Quercetin hexose–glucuronide
						303.0515	$[Y_0]^+$				301.0360	$[Y_0]^-$	
											135.0432	$[^{0,2}A–CO]^{-};[^{0,2}B]^-$	
68	10.58	–	641.1385	3.1	$C_{27}H_{29}O_{18}$	663.1232	$[M+Na]^+$	639.1168	–2.9	$C_{27}H_{27}O_{18}$	463.0865	$[Y_1]^-$	Quercetin hexose–glucuronide
						465.1066	$[Y_1]^+$				301.0360	$[Y_0]^-$	
						303.0515	$[Y_0]^+$						
69	21.52	255, 352	551.1039	0.2	$C_{24}H_{23}O_{15}$	573.0847	$[M+Na]^+$	549.0879	–0.1	$C_{24}H_{21}O_{15}$	1099.1829	$[2M–H]^-$	Quercetin–3–*O*–malonylglucoside
						303.0508	$[Y_0]^+$				505.0987	$[M–H–CO_2]^-$	
						229.0497	$[Y_0–CHO–OH–CO]^+$				463.0865	$[M–H–CO_2–C2H_2O]^-$	
						153.0186	$[^{1,3}A]^+$				301.0340	$[Y_0]^-$	
						145.0516	$[Y_0–CHO–OH–4CO]^+$				300.0273	$[Y_0–H]^-$	
											255.0305	$[Y_0–CHO–OH]^-$	
											151.0038	$[^{1,3}A]^-$	
70	22.03	252, 364	551.1031	–0.6	$C_{24}H_{23}O_{15}$	573.0846	$[M+Na]^+$	549.0891	1.1	$C_{24}H_{21}O_{15}$	505.0990	$[M–H–CO_2]^-$	Quercetin–3–*O*–malonylglucoside
						303.0506	$[Y_0]^+$				463.0880	$[M–H–CO_2–C2H_2O]^-$	
						229.0504	$[Y_0–CHO–OH–CO]^+$				301.0351	$[Y_0]^-$	
						153.0196	$[^{1,3}A]^+$				255.0284	$[Y_0–CHO–OH]^-$	
						145.0495	$[Y_0–CHO–OH–4CO]^+$				151.0033	$[^{1,3}A]^-$	
											107.0130	$[^{0,2}A–2CO]^{-};[^{0,2}B–CO]^-$	
71	23.69	–	551.1041	0.4	$C_{24}H_{23}O_{15}$	573.0851	$[M+Na]^+$	549.0894	1.4	$C_{24}H_{21}O_{15}$	505.0980	$[M–H–CO_2]^-$	Quercetin–3–*O*–malonylglucoside
						303.0504	$[Y_0]^+$				301.0335	$[Y_0]^-$	
						229.0488	$[Y_0–CHO–OH–CO]^+$				300.0266	$[Y_0–H]^-$	
						153.0195	$[^{1,3}A]^+$				255.0290	$[Y_0–CHO–OH]^-$	
											151.0039	$[^{1,3}A]^-$	
											107.0127	$[^{0,2}A–2CO]^{-};[^{0,2}B–CO]^-$	
72	11.51	253, 355	727.1348	–1.0	$C_{30}H_{31}O_{21}$	749.1142	$[M+Na]^+$	725.1176	–2.5	$C_{30}H_{29}O_{21}$	681.1274	$[M–H–CO_2]^-$	Quercetin–3–*O*–(6''–*O*–malonyl)–glucoside–7–*O*–glucuronide
						479.0830	$[Y_1]^+$				505.0977	$[M–H–CO_2–glucuronyl]^-$	

	LC	DAD	ESI(+)–QToF/MS					ESI(–)–QToF/MS					Assignment
Nº	Rt (min)	UV bands (nm)	Exp. Acc. Mass $[M+H]^+$	Error (mDa)	Formula $[M+H]^+$	Adducts & fragment ions of $[M+H]^+$ *m/z*		Exp. Acc. Mass $[M-H]^-$	Error (mDa)	Formula $[M-H]^-$	Adducts & fragment ions of $[M-H]^-$ *m/z*		Tentative identification
						303.0494	$[Y_0]^+$				301.0355	$[Y_0]^-$	
											255.0300	$[Y_0–CHO–OH]^-$	
73	13.82	253, 350	713.1565	0.0	$C_{30}H_{33}O_{20}$	735.1379	$[M+Na]^+$	711.1411	0.2	$C_{30}H_{31}O_{21}$	667.1519	$[M–H–CO_2]^-$	Quercetin–3–*O*–(6"–*O*–malonyl)–glucoside–7–*O*–glucoside
						465.1039	$[Y_1]^+$				463.0863	$[M–H–CO_2–hexosyl–C_2H_2O]^-$	
						303.0508	$[Y_0]^+$				301.0348	$[Y_0]^-$	
											135.0641	$[^{0,2}A–CO]^-$;$[^{0,2}B]^-$	
74	12.18	–	627.1580	1.9	$C_{27}H_{31}O_{17}$	649.1414	$[M+Na]^+$	625.1391	–1.4	$C_{27}H_{29}O_{17}$	463.0874	$[Y_1]^-$	Quercetin–*O*–di–hexoside
						303.0502	$[Y_0]^+$				301.0344	$[Y_0]^-$	
						137.0611	$[^{0,2}A–CO]^+$						
75	16.07	–	627.1556	–0.5	$C_{27}H_{31}O_{17}$	649.1367	$[M+Na]^+$	625.1400	–0.5	$C_{27}H_{29}O_{17}$	447.0833	$[Y_1]^-$	Quercetin–*O*–rhamnosyl–gluconide
						449.1805	$[Y_1]^+$				301.0290	$[Y_0]^-$	
						303.0522	$[Y_0]^+$						
76	25.27	265, 347	535.1094	0.6	$C_{24}H_{23}O_{14}$	557.0905	$[M+Na]^+$	533.0889	–3.9	$C_{24}H_{21}O_{14}$	489.1039	$[M–H–CO_2]^-$	Kaempferol–3–*O*–(6"–*O*–malonyl)–glucoside
						287.0560	$[Y_0]^+$				285.0399	$[Y_0]^-$	
						121.0301	$[^{0,2}B]^+$				255.0298	$[Y_0–CO–2H]^-$	
						153.0204	$[^{1,3}A]^+$				227.0343	$[Y_0–CHO–CO–H]^-$	
											151.0037	$[^{1,3}A]^-$	
											107.0154	$[^{0,2}A–2CO]^-$;$[^{0,2}B–CO]^-$	
77	23.90	–	449.1092	0.8	$C_{21}H_{21}O_{11}$	471.0901	$[M+Na]^+$	447.0925	0.2	$C_{21}H_{19}O_{11}$	285.0410	$[Y_0]^-$	Kampferol–3–*O*–glucoside
						287.0561	$[Y_0]^+$				151.0056	$[^{1,3}A]^-$	
78	26.43	–	449.1084	0.0	$C_{21}H_{21}O_{11}$	471.0830	$[M+Na]^+$	447.0925	–0.1	$C_{21}H_{19}O_{11}$	285.0406	$[Y_0]^-$	Kaempferol–hexoside
						287.0549	$[Y_0]^+$						
79	22.34	265, 332	463.0878	0.1	$C_{21}H_{19}O_{12}$	485.0683	$[M+Na]^+$	461.0724	0.4	$C_{21}H_{17}O_{12}$	285.0403	$[Y_0]^-$	Kaempferol–3–*O*–glucuronide
						287.0559	$[Y_0]^+$				257.0471	$[Y_0–CO]^-$	
						133.1025	$[^{1,3}B–2H]^+$				229.0509	$[Y_0–2CO]^-$	
80	27.08	–	287.0560	0.4	$C_{15}H_{11}O_6$	259.1070	$[Y_0–CO]^+$	285.0399	0.0	$C_{15}H_9O_6$	153.0197	$[^{1,3}A]^-$	Kaempferol
						213.0885	$[Y_0–H_2O–2CO]^+$				137.0239	$[^{0,2}A–CO]^-$;$[^{0,2}B]^-$	
						185.0970	$[Y_0–H_2O–3CO]^+$				133.0310	$[^{1,3}B–2H]^-$	
						171.0856	$[Y_0–CHO–OH–CO–C2H_2O]^+$				109.0296	$[^{0,2}A–2CO]^-$;$[^{0,2}B–CO]^-$	
						153.0146	$[^{1,3}A]^+$				93.0340	$[^{0,2}B–CO]^-$	
						137.0894	$[^{0,2}A–CO]^+$;$[^{0,2}B]^+$						
						135.0776	$[^{1,3}B–2H]^+$						
						127.0807	$[Y_0–CHO–OH–3CO–CH_2O]^+$						
						121.0653	$[^{0,2}B]^+$						
						107.0500	$[^{1,3}A–H_2O–CO]^+$, $[^{1,3}B–CO]^+$						
						105.0681	$[^{1,3}B–2H–CO]^+$						
Flavones													
81	19.82	255, 347	449.1081	–0.3	$C_{21}H_{21}O_{11}$	471.0901	$[M+Na]^+$	447.0925	–0.2	$C_{21}H_{19}O_{11}$	895.1951	$[2M–H]^-$	Luteolin–7–*O*–glucoside
						287.0559	$[Y_0]^+$				285.0400	$[Y_0]^-$	
						153.0177	$[^{1,3}A]^+$				217.0505	$[Y_0–C2H_2O–C2H_2]^-$	
						135.0821	$[^{1,3}B]^+$				199.0396	$[Y_0–CHO–2CO–H]^-$	
82	17.45	253, 348	463.0880	0.3	$C_{21}H_{19}O_{12}$	485.0690	$[M+Na]^+$	461.0717	–0.3	$C_{21}H_{17}O_{12}$	923.1496	$[2M–H]^-$	Luteolin 7–*O*–glucuronide
						287.0559	$[Y_0]^+$				285.0398	$[Y_0]^-$	
						153.0186	$[^{1,3}A]^+$				217.0506	$[Y_0–C2H_2O–C2H_2]^-$	
											199.0390	$[Y_0–CHO–2CO–H]^-$	
											151.0032	$[^{1,3}A]^-$	
											133.0287	$[^{1,3}B]^-$	
83	20.27	–	595.1651	–1.2	$C_{27}H_{31}O_{15}$			593.1498	–0.8	$C_{27}H_{29}O_{15}$	285.0685	$[Y_0]^-$	Luteolin–7–*O*–rhamnosyl–hexoside

	LC	DAD	ESI(+)–QToF/MS					ESI(–)–QToF/MS					Assignment
Nº	Rt (min)	UV bands (nm)	Exp. Acc. Mass $[M+H]^+$	Error (mDa)	Formula $[M+H]^+$	Adducts & fragment ions of $[M+H]^+$ *m/z*		Exp. Acc. Mass $[M-H]^-$	Error (mDa)	Formula $[M-H]^-$	Adducts & fragment ions of $[M-H]^-$ *m/z*		Tentative identification
84	21.17	268, 351	595.1672	0.9	$C_{27}H_{31}O_{15}$	617.1484	$[M+Na]^+$	593.1498	–0.8	$C_{27}H_{29}O_{15}$	447.0604	$[Y_1]^-$	Luteolin–7–*O*–rutinoside
						449.1083	$[Y_1]^+$				285.0400	$[Y_0]^-$	
						287.0557	$[Y_0]^+$						
85	11.85	265, 339	553.1192	-0.1	$C_{24}H_{25}O_{15}$	1069.2104	$[2(M–H_2O)+H]^+$	551.1027	-1.0	$C_{24}H_{23}O_{15}$	1103.2147	$[2M-H]^-$	Luteolin–hydroxymalonylhexoside
						575.1013	$[M+Na]^+$				507.1135	$[M–H–CO_2]^-$	
						535.1091	$[M+H–H_2O]^+$				371.0977	$[M–H–hex]^-$	
						449.0679	$[M–OH–malonyl+H]^+$				285.0402	$[Y_0]^-$	
						287.0556	$[Y_0]^+$				241.0501	$[Y_0–CO2]^-$	
						137.0244	$[^{0,2}A–CO]^+;[^{0,2}B]^+$				255.0302	$[Y_0–CO–2H]^-$	
											227.0341	$[Y_0–CHO–CO–H]^-$	
											199.0396	$[Y_0–CHO–2CO–H]^-$	
86	20.57	–	447.0912	1.5	$C_{21}H_{19}O_{11}$	271.0608	$[Y_0]^+$	445.0763	0.8	$C_{21}H_{17}O_{11}$	269.0449	$[Y_0]^-$	Apigenin–glucuronide
87	23.02	259, 328	433.1137	–0.2	$C_{21}H_{21}O_{10}$	271.0610	$[Y_0]^+$	431.0972	0.6	$C_{21}H_{19}O_{10}$	269.0441	$[Y_0]^-$	Apigenin–glucoside
88	23.90	–	579.1711	0.3	$C_{21}H_{21}O_{10}$	433.1124	$[Y_1]^+$	577.1553	0.4	$C_{27}H_{29}O_{14}$	433.2084	$[Y_1]^-$	Apigenin–*O*–rhamnosyl–hexoside
						271.0605	$[Y_0]^+$				269.0446	$[Y_0]^-$	
89	14.92		465.1038	0.5	$C_{21}H_{21}O_{12}$	487.0856	$[M+Na]^+$	463.0872	-0.5	$C_{21}H_{19}O_{12}$	269.0446	$[Y_0]^-$	Apigenin–pentahydroxyhexanoide
						271.0606	$[Y_0]^+$						
						163.0387	$[^{0,4}B]^+$						
						153.0191	$[^{1,3}A]^+$						
						145.0296	$[^{0,4}B–H_2O]^+$						
						121.0292	$[^{0,2}B]^+$						
						91.0529	$[^{1,3}B]^+$						
90	26.99	–	839.3358	–2.0	$C_{40}H_{55}O_{19}$	271.0610	$[Y_0]^+$	837.3194	–1.3	$C_{40}H_{53}O_{19}$	269.0450	$[Y_0]^-$	Apigenin conjugate
91	27.08	–	287.0560	0.4	$C_{15}H_{11}O_6$	259.1070	$[Y_0–CO]^+$	285.0399	0.0	$C_{15}H_9O_6$	153.0197	$[^{1,3}A]^-$	Luteolin
						213.0885	$[Y_0–H_2O–2CO]^+$				137.0239	$[^{0,2}A–CO]^-;[^{0,2}B]^-$	
						185.0970	$[Y_0–H_2O–3CO]^+$						
						179.0649	$[^{0,4}B]^+$						
						153.0146	$[^{1,3}A]^+$						
						137.0894	$[^{0,2}A–CO]^+;[^{0,2}B]^+$						
						135.0776	$[^{0,2}B–2H]^+$						
						117.0767	$[^{1,3}B–H_2O]^+$						
						107.0500	$[^{1,3}A–H_2O–CO]^+$, $[^{1,3}B–CO]^+$						
Flavanones													
92	14.87	284, 329 sh	465.1026	–0.7	$C_{21}H_{21}O_{12}$	487.0830	$[M+Na]^+$	463.0882	0.5	$C_{21}H_{19}O_{12}$	287.0555	$[Y_0]^-$	Eriodictyo–*O*–glucuronide
						289.0715	$[Y_0]^+$				285.0407	$[Y_0–2H]^-$	
						153.0187	$[^{1,3}A]^+$				151.0037	$[^{1,3}A]^-$	
											135.0452	$[^{1,3}B]^-$	
											107.0133	$[^{0,4}A]^-$	
Anthocyanidin													
93	10.80		449.1079	0.5	$C_{21}H_{20}O_{11}$	287.0558	$[Y_0]^+$	-	-	$C_{21}H_{21}O_{11}$			Cyanidin–3–*O*–glucoside
						213.0555	$[Y_0–H_2O–2CO]^+$						
						185.0208	$[Y_0–H_2O–3CO]^+$						
						137.0251	$[^{0,2}B]^+$						
						121.0298	$[^{0,3}A]^+$						
						109.0309	$[^{0,2}B–CO]^+$						
94	13.62		535.1089	-0.1	$C_{24}H_{23}O_{14}$	287.0556	$[Y_0]^+$	-	-	$C_{24}H_{23}O_{14}$	507.1121	$[M–CO]^-$	Cyanidin–3–*O*–(3''–O–malonyl)–glucoside
						137.0236	$[^{0,2}B]^+$				489.1013	$[M–CO–H_2O]^-$	

	LC	DAD	ESI(+)–QToF/MS					ESI(–)–QToF/MS					Assignment
Nº	**Rt (min)**	**UV bands (nm)**	**Exp. Acc. Mass $[M+H]^+$**	**Error (mDa)**	**Formula $[M+H]^+$**	**Adducts & fragment ions of $[M+H]^+$**		**Exp. Acc. Mass $[M-H]^-$**	**Error (mDa)**	**Formula $[M-H]^-$**	**Adducts & fragment ions of $[M-H]^-$**		**Tentative identification**
						m/z					***m/z***		
						109.0292	$[^{0,2}B–CO]^+$				285.0390	$[Y_0–2H]^-$	
95	16.84	279, >500	535.1095	-0.7	$C_{24}H_{23}O_{14}$	287.0561	$[Y_0]^+$	-	-	$C_{24}H_{23}O_{14}$	507.1138	$[M–CO]^-$	Cyanidin–3–*O*–(6''–O–malonyl)–glucoside
						213.0555	$[Y_0–H_2O–2CO]^+$				489.1035	$[M–CO–H_2O]^-$	
						137.0246	$[^{0,2}B]^+$				461.0728	$[M–2CO–H_2O]^-$	
						109.0293	$[^{0,2}B–CO]^+$				285.0400	$[Y_0–2H]^-$	
96	20.25		491.1166	2.4	$C_{23}H_{23}O_{12}$	449.1080	$[M–CH_2CO]^+$	-	-	$C_{24}H_{23}O_{14}$			Cyanidin–3–*O*–(6''–O–acetyl)–glucoside
						287.0559	$[Y_0]^+$						
						269.0442	$[Y_0–H_2O]^+$						
						259.0596	$[Y_0–CO]^+$						

[a] See footnotes in Table 1.

Table 3. Retention times, UV-visible maxima and MS^E data of coumarins, hydrolysable tannins and lignans identified by UHPLC-DAD-ESI-Q-ToF/MS in oak leaf lettuce cultivars.[a]

	LC	DAD	ESI(+)–QToF/MS					ESI(–)–QToF/MS					Assignment
Nº	Rt (min)	UV bands (nm)	Exp. Acc. Mass $[M+H]^+$	Error (mDa)	Formula $[M+H]^+$	Adducts & fragment ions of $[M+H]^+$ *m/z*		Exp. Acc. Mass $[M-H]^-$	Error (mDa)	Formula $[M-H]^-$	Adducts & fragment ions of $[M-H]^-$ *m/z*		Tentative identification
Coumarins													
97	6.50	290, 340	341.0866	–0.7	$C_{15}H_{17}O_9$	363.0684	$[M+Na]^+$	339.0727	1.1	$C_{15}H_{15}O_9$	399.1273	$[M-H+AcO]^-$	Esculetin–6–*O*–glucoside
						179.0345	$[Y_0]^+$				177.0188	$[Y_0]^-$	
						133.0284	$[Y_0-CO-H_2O]^+$				133.0288	$[Y_0-CO_2]^-$	
						123.0456	$[Y_0-2CO]^+$				105.0336	$[Y_0-CO_2-CO]^-$	
98	7.31	–	179.0341	0.3	$C_9H_7O_4$	133.0292	$[M+H-CO-H_2O]^+$	177.0191	–0.3	$C_9H_5O_4$	149.0236	$[M-CO]^-$	Dihydroxycoumarin
						123.0437	$[M+H-2CO]^+$				133.0288	$[M-CO_2]^-$	
											105.0341	$[M-CO_2-CO]^-$	
99	10.23	–	179.0344	0.0	$C_9H_7O_4$	133.0289	$[M+H-CO-H_2O]^+$	177.0192	–0.4	$C_9H_5O_4$	149.0222	$[M-CO]^-$	Dihydroxycoumarin
						123.0452	$[M+H-2CO]^+$				133.0292	$[M-CO_2]^-$	
											105.0344	$[M-CO_2-CO]^-$	
100	12.02	296, 330	179.0339	0.0	$C_9H_7O_4$	133.0288	$[M+H-CO-H_2O]^+$	177.0187	0.1	$C_9H_5O_4$	133.0236	$[M-CO_2]^-$	6,7–dihydroxycoumarin
						123.0421	$[M+H-2CO]^+$				105.0340	$[M-CO_2-CO]^-$	
101	9.05	–	295.0518	–6.4	$C_{13}H_{11}O_8$	317.0241	$[M+Na]^+$	293.0295	0.2	$C_{13}H_9O_8$	177.0194	$[Y_0]^-$	Maloyl–dihydroxycoumarin
						179.0376	$[Y_0]^+$				149.0243	$[Y_0-CO]^-$	
						133.0286	$[Y_0-CO-H_2O]^+$				133.0284	$[Y_0-CO_2]^-$	
						123.0463	$[Y_0-2CO]^+$				105.0342	$[Y_0-CO_2-CO]^-$	
102	10.54	–	295.0510	–5.6	$C_{13}H_{11}O_8$	133.0288	$[Y_0-CO-H_2O]^+$	293.0296	0.1	$C_{13}H_9O_8$	177.0187	$[Y_0]^-$	Maloyl–dihydroxycoumarin
											149.0090	$[Y_0-CO]^-$	
											133.0286	$[Y_0-CO_2]^-$	
											105.0339	$[Y_0-CO_2-CO]^-$	
103	12.54	–	295.0541	–8.7	$C_{13}H_{11}O_8$	179.0348	$[Y_0]^+$	293.0299	–0.2	$C_{13}H_9O_8$	177.0189	$[Y_0]^-$	Maloyl–dihydroxycoumarin
						133.0446	$[Y_0-CO-H_2O]^+$				149.0139	$[Y_0-CO]^-$	
											133.0290	$[Y_0-CO_2]^-$	
											105.0343	$[Y_0-CO_2-CO]^-$	
Hydrolysable tannins													
104	27.09	–			$C_{30}H_{31}O_{12}$			581.1663	–0.4	$C_{30}H_{29}O_{12}$	295.0826	[4–hydroxyphenylacetichex–H–H_2O]$^-$	Tri–4–hydroxyphenylacetic acid–glucoside
											175.0391	[4–hydroxyphenylacetichex–H–H_2O–$C_6H_5CH_3CO$]$^-$	
											151.0392	[4-hydroxyphenylacetic–H]$^-$	
											143.0344	[4–hydroxyphenylacetichex–H–H_2O–$C_6H_5CH_2OHCO_2$]$^-$	
Lignan derivatives													
105	13.90	–			$C_{28}H_{37}O_{13}$	603.2055	$[M+Na]^+$	579.2075	0.3	$C_{28}H_{35}O_{13}$	417.1544	$[M-H-hexosyl]^-$	Syringaresinol–hexose
						383.1479	$[M+H-hexosyl-2H_2O]^+$				399.1437	$[M-H-hexosyl-H_2O]^-$	
106	18.97	–			$C_{28}H_{37}O_{13}$			579.2104	–2.6	$C_{28}H_{35}O_{13}$			Syringaresinol–hexose
107	19.63	–			$C_{28}H_{37}O_{13}$	603.2061	$[M+Na]^+$	579.2079	–0.1	$C_{28}H_{35}O_{13}$	417.1558	$[M-H-hexosyl]^-$	Syringaresinol–hexose
											399.1493	$[M-H-hexosyl-H_2O]^-$	
108	23.30	–			$C_{28}H_{37}O_{13}$	603.2059	$[M+Na]^+$	579.2075	0.3	$C_{28}H_{35}O_{13}$	417.1555	$[M-H-hexosyl]^-$	Syringaresinol–hexose
						383.1505	$[M+H-hexosyl-2H_2O]^+$				387.1104	$[M-H-hexosyl-2CH_3]^-$	
109	15.06	205, 280			$C_{30}H_{39}O_{14}$			621.2198	–1.5	$C_{30}H_{37}O_{14}$	417.1559	$[M-H-acetylhexosyl]^-$	Syringaresinol–acetylhexose
											402.1313	$[M-H-acetylhexosyl-CH_3]^-$	
											399.1447	$[M-H_2O]^-$	
											387.1058	$[M-H-2CH_3]^-$	
110	24.50	–			$C_{30}H_{39}O_{14}$			621.2183	0.0	$C_{30}H_{37}O_{14}$	417.1548	$[M-H-acetylhexosyl]^-$	Syringaresinol–acetylhexose

	LC	DAD	ESI(+)–QToF/MS				ESI(–)–QToF/MS				Assignment
Nº	Rt (min)	UV bands (nm)	Exp. Acc. Mass $[M+H]^+$	Error (mDa)	Formula $[M+H]^+$	Adducts & fragment ions of $[M+H]^+$ *m/z*	Exp. Acc. Mass $[M-H]^-$	Error (mDa)	Formula $[M-H]^-$	Adducts & fragment ions of $[M-H]^-$ *m/z*	Tentative identification
										402.1313 $[M-H-acetylhexosyl-CH_3]^-$	
										387.1078 $[M-H-acetylhexosyl-2CH_3]^-$	
										359.1111 $[M-H-acetylhexosyl-2CH_3-CO]^-$	
										181.0503 $[M-H-acetylhexosyl-2CH_3O-OH-C_6H_2-CHO-CH_2CHCHCH_2]^-$	
										166.0268 $[M-H-acetylhexosyl-2CH_3O-C_6H_2O-CHO-CH_2CHCHCH_2O]^-$	
										151.0044 $[M-H-acetylhexosyl-2CH_3O-OH-C_6H_2-2CHO-CH_2CHCHCH_2-H]^-$	
										123.0065 $[M-H-acetylhexosyl-2CH_3O-C_6H_2O-2CHO-CH_2CHCHCH_2-CH_3O]^-$	
111	24.63	–			$C_{30}H_{39}O_{14}$		621.2181	0.2	$C_{30}H_{37}O_{14}$	417.1546 $[M-H-acetylhexosyl]^-$	Syringaresinol–acetylhexose
										402.1313 $[M-H-acetylhexosyl-CH_3]^-$	
										387.1074 $[M-H-acetylhexosyl-2CH_3]^-$	
										359.1084 $[M-H-acetylhexosyl-2CH_3-CO]^-$	
										181.0503 $[M-H-acetylhexosyl-2CH_3O-OH-C_6H_2-CHO-CH_2CHCHCH_2]^-$	
										166.0269 $[M-H-acetylhexosyl-2CH_3O-C_6H_2O-CHO-CH_2CHCHCH_2O]^-$	
										151.0041 $[M-H-acetylhexosyl-2CH_3O-OH-C_6H_2-2CHO-CH_2CHCHCH_2-H]^-$	
112	19.22	–			$C_{28}H_{39}O_{13}$		581.2239	–0.5	$C_{28}H_{37}O_{13}$	341.1392 $[M-H-hexosyl-CH_3COOH-H_2O]^-$	Dimethoxy–hexosyl–lariciresinol
										329.1390 $[M-H-hexosyl-CH_3COOH-2CH_3]^-$	
113	19.39	–			$C_{28}H_{39}O_{13}$		581.2238	–0.4	$C_{28}H_{37}O_{13}$	359.1494 $[M-H-hexosyl-CH_3COOH]^-$	Dimethoxy–hexosyl–lariciresinol
										341.1383 $[M-H-hexosyl-CH_3COOH-H_2O]^-$	
										329.1392 $[M-H-hexosyl-CH_3COOH-2CH_3]^-$	
114	19.82	–			$C_{28}H_{39}O_{13}$		581.2201	3.3	$C_{28}H_{37}O_{13}$	359.1445 $[M-H-hexosyl-CH_3COOH]^-$	Dimethoxy–hexosyl–lariciresinol
										329.1392 $[M-H-hexosyl-CH_3COOH-2CH_3]^-$	
115	16.37	–			$C_{34}H_{49}O_{18}$		743.2742	2.0	$C_{34}H_{47}O_{18}$	581.2249 $[M-H-hexosyl]^-$	Dimethoxy–dihexosyl–lariciresinol
										359.1494 $[M-H-2hexosyl-CH_3COOH]^-$	
										341.1383 $[M-H-2hexosyl-CH_3COOH-H_2O]^-$	
										329.1392 $[M-H-2hexosyl-CH_3COOH-2CH_3]^-$	

[a] See footnotes in Table 1.